

Multi-User Full-Duplex Relaying: Enabling Dual Connectivity via Impairments-Aware Successive Interference Cancellation

Vimal Radhakrishnan, *Student Member, IEEE*, Omid Taghizadeh, *Member, IEEE*,
Rudolf Mathar, *Senior Member, IEEE*

Abstract—In this paper, we consider the downlink of a cellular communication network, where dual-connectivity (DuC) at the end-users is enabled with the assistance of a full-duplex (FD) massive-multiple-input-multiple-output (mMIMO) relay. In particular, the base station (BS) transmits separate data streams through the co-channel direct link as well as the FD relay channel, utilizing the successive-interference-cancellation (SuIC) capability at the receiver. As a result, the downlink communication data can be interchangeably loaded to separate sub-carriers, employing an orthogonal multi-carrier (MC) strategy, or to different available links, i.e., direct or FD relay link, employing the non-orthogonal SuIC at the receiver. In order to reliably model the SuIC operation at the receiver, the collective sources of impairments, including the non-linear transmit and receiver chain distortions as well as the channel state information (CSI) inaccuracy are incorporated. An optimization problem for joint sub-carrier and power allocation is then devised in order to maximize system weighted sum-rate, which belongs to the class of smooth difference-of-convex (DC) problems. An iterative optimization solution is then proposed, utilizing successive inner approximation (SIA) framework, which converges to the point that satisfies Karush–Kuhn–Tucker optimality conditions. Numerical results show performance and robustness gain of proposed SuIC scheme in terms of sum-rate compared to previously proposed single-connectivity and half-duplex relaying schemes.

Keywords—Massive MIMO, Full duplex, Dual connectivity, Multi-carrier, Imperfect CSI, Successive interference cancellation

I. INTRODUCTION

Dual-connectivity (DuC) is proposed by 3rd Generation Partnership Project (3GPP) in the long term evolution (LTE) Release 12 specification as a promising approach to achieve higher per-user throughput, mobility robustness, and load balancing [2]. It allows a user terminal to simultaneously transmit and receive data from two cell groups via a master evolved Node-B (eNodeB) and a secondary eNodeB, which operate on different carrier frequencies and are interconnected by traditional backhaul links. In order to manage the coexisting access links at separate time/frequency blocks, the mixed

orthogonal frequency division multiplexing (mixed-OFDM) has been selected as the multiple access technique for the upcoming fifth-generation (5G) networks [3], [4].

Various non-orthogonal multiple access (NOMA) schemes have been also proposed to improve the performance of the system in terms of spectral efficiency as well as to support a massive number of dramatically different classes of users and applications. In contrast to conventional orthogonal multiplexing schemes, where multiple users are served in orthogonal frequency or time domains, NOMA schemes serve more than one user in the same frequency-time resource block by multiplexing users in other domains such as the power domain or code domain. Power domain NOMA as well as rate-splitting (RS) is implemented using the successive-interference-cancellation (SuIC) approach at the receiver. In a two-level SuIC approach, during the first phase, the received signal is processed by acknowledging the strong signal as the desired signal while treating the rest of the received signal as noise. During the second phase, the receiver processes the received signal after removing the known part of the signal, the strong signal, which in turn reduces the total interference [5]. A brief overview of DuC technology considering the integration between fourth-generation (4G) and 5G cellular networks have been the focus of [6]–[8], whereas the applications of DuC for LTE communication networks have been investigated in [2], [9], [10]. In [6], the authors also present open issues and promising use-cases such as user-cell association, the interaction between base-stations, and resource allocation in the related scenarios. The utilization of the SuIC schemes, as an enabling element for user DuC, as well as the improvement of the system performance has been investigated in [5], [11]–[13].

In a parallel track of study, full-duplex (FD) massive-multiple-input-multiple-output (mMIMO) communication systems have been studied in [14]–[21], from the aspects of implementation, system performance analysis and resource allocation. In particular, an FD relay has the capability to transmit and receive at the same time and frequency, thereby improving the performance of the traditionally half-duplex (HD) relays from the aspects of spectral efficiency and the end-to-end latency [14]. Nevertheless, the potential gains of employing an FD transceiver is accompanied by accepting a higher processing and implementation complexity, associated with the required additional signal processing for self-interference cancellation (SIC) as well as the higher implemen-

V. Radhakrishnan and R. Mathar are with the Institute for Theoretical Information Technology, RWTH Aachen University, Aachen, 52074, Germany (email: {radhakrishnan, mathar}@ti.rwth-aachen.de).

O. Taghizadeh is with the Network Information Theory Group, Technische Universität Berlin, 10587 Berlin, Germany (email: {taghizadehmotlagh}@tu-berlin.de). This work has been supported by Deutsche Forschungsgemeinschaft (DFG), under the Grant No. MA 1184/38 – 1.

Part of this work has been presented in WSA 2020, 24nd International ITG Workshop on Smart Antennas [1].

tation cost. In particular, FD systems suffer from an imperfect SIC, i.e., interference from their own transmission, as well as the co-channel interference from the direct source-destination channel. In this regard, the application of FD mMIMO relaying has been studied, e.g., in [14], [15], [20], from the aspects of system performance analysis and resource allocation. However, while the direct source-to-destination channel, co-existing with the FD relay channel, can be also viewed as a parallel information link, it has been considered merely as a source of interference in the previous works. Furthermore, while the impact of non-linear hardware impairments have been generally found to be significant in FD mMIMO systems¹, such impact, leading to residual self-interference (RSI) and inter-carrier leakage (ICL), has been generally ignored in the study of multi-carrier (MC) FD mMIMO networks.

In this work, we aim at closing the aforementioned gap by studying a multi-user cellular system in the downlink, where DuC between the base-station (BS) and user terminals are enabled at the same carrier frequency with the aid of a decode-and-forward (DF) FD mMIMO relay. The main contributions of this paper are summarized as following:

- In contrast to [14], [15], [20], [21], where the direct channel has been ignored or merely considered as an interference channel in the context of DF FD mMIMO relaying, or to [9], [10] where DuC is enabled by concurrently enabling links at strictly separate frequency bands, in this work we study a system where an mMIMO BS transmits separate data streams through the direct and FD relay channels, hence enabling co-channel DuC by utilizing SuIC capability at the receiver. In this regard, the downlink communication data can be interchangeably loaded to separate sub-carriers, employing an orthogonal multi-carrier strategy, or to the different available links, i.e., direct or the FD relay link, employing the non-orthogonal SuIC reception at the receiver.
- In order to enable a successful SuIC scheme for the employed multi-carrier system, we consider the impact of the imperfect channel state information (CSI), as well as non-linear hardware distortion at the studied FD mMIMO MC link, which leads to RSI and ICL at the relay. In this regard, we extend the available frequency domain characterization of the distortion signals, given in [22], specialized for CP-OFDM system, to a general MC system with orthogonal waveforms. This generalizes the studied framework for different multi-carrier strategies, e.g., orthogonal variable spreading factor (OVSF)-Code Division Multiple Access (CDMA) and the variations of OFDMA.
- An optimization problem for joint sub-carrier and power allocation is then devised in order to maximize the system sum-rate, which belongs to the class of smooth difference-of-convex (DC) optimization problems. An iterative optimization solution is then proposed, utilizing the successive inner approximation (SIA) frame-

¹This is both due to the strong self-interference channel as well as the low-resolution nature of the hardware elements which are usually associated with the large antenna array dimension.

work [23], which converges to the point that satisfies Karush–Kuhn–Tucker (KKT) optimality conditions.

Numerical results show performance and robustness gain of our proposed SuIC scheme in terms of sum-rate compared to the previously proposed single-connectivity and HD schemes.

In Section II, the studied system model is presented. In Section III, the proposed design strategies and the associated optimization problems are studied. In Section V-B, using numerical simulations, we evaluate the performance of our proposed designs. The main findings and insights are summarized in Section VI.

A. Mathematical Notation

Throughout this paper, we denote the vectors and matrices by lower-case and upper-case bold letters, respectively. We use $\mathbb{E}\{\cdot\}$, $|\cdot|$, $\text{Tr}(\cdot)$, $(\cdot)^{-1}$, $(\cdot)^*$, $(\cdot)^T$, and $(\cdot)^H$ for mathematical expectation, determinant, trace, inverse, conjugate, transpose, and Hermitian transpose, respectively. We use $\text{diag}(\cdot)$ for the diag operator, which returns a diagonal matrix by setting off-diagonal elements to zero. We denote an all zero matrix of size $m \times n$ by $\mathbf{0}_{m \times n}$. A complex Gaussian distribution with mean \mathbf{a} and variance \mathbf{A} is denoted as $\mathcal{CN}(\mathbf{a}, \mathbf{A})$. We represent the Euclidean norm as $\|\cdot\|_2$. We denote the set of real, positive real, and complex numbers as \mathbb{R} , \mathbb{R}^+ , and \mathbb{C} respectively. $\delta_{ij} = 1$ when $i = j$ and $\delta_{ij} = 0$ otherwise.

II. SYSTEM MODEL AND ANALYSIS

A. Setup Description

We consider a relay-assisted MC downlink communication between an mMIMO BS and L downlink users, which are connected to the BS through the direct link as well as the FD relay link. The BS uses the DuC (similar to NOMA/RS) approach to communicate with the user directly and also using an FD DF relay. In this regard, two messages, both transmitted from the BS and destined for the same user, are precoded separately and simultaneously transmitted; one through the direct link (DL) and one through the relay link (RL). At the user end, the received signal is processed in two phases using the SuIC technique. In the first phase, the received signal from the BS is treated as noise while considering the strong received signal from the relay as the desired signal. In the second phase, as the received signal from the relay becomes known, this part can be removed from the received signal, which reduces the total interference.

Let N_{BS} be the number of transmit antennas at the BS node. We consider that the relay is equipped with a single directive² receive antenna, which serve the fronthaul link and N_r transmit

²This is practical, since both the location of the BS node and the relay nodes are usually known and static. Since the channel between the BS and relay is static and enjoys a line of sight (LOS) condition, the LOS signal part becomes dominant which constitutes the rank of the channel to be almost one. Please note that the main advantage of the programmable multi-antenna (MIMO) systems are the non-static, i.e., mobile scenarios (e.g., in the BS-user and relay-user links where a MIMO setup is considered, or when the channel is of full-rank nature and hence a significant multiplexing gain can be obtained). In the static BS-relay link, a directive antenna helps to take complete advantage for this LOS channel and thereby receives the dominant part of the signal.

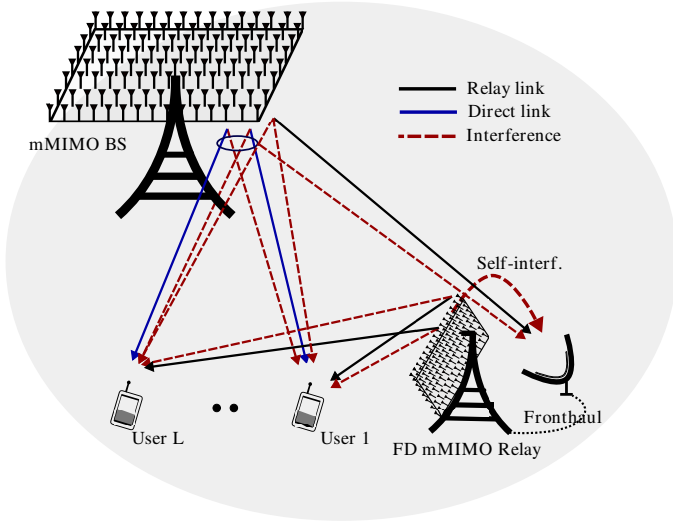


Fig. 1. The studied multi-user FD relaying scenario, where users dual connectivity is enabled via the direct as well as the relay links.

antennas, which serve the relay-user communications. Nevertheless, due to the FD capability at the relay node, the fronthaul link as well as the relay-user links coexist at the same channel resource, i.e., time and frequency. The schematic of the studied multi-user FD relaying-enabled DuC system depicted in Fig. 1.

In this paper, we denote the index set of all sub-carriers and downlink users by \mathbb{K} and \mathbb{L} , respectively. Furthermore, $\mathbf{h}_{\text{sd}}^{i,k} \in \mathbb{C}^{1 \times N_{\text{BS}}}$ and $\mathbf{h}_{\text{rd}}^{i,k} \in \mathbb{C}^{1 \times N_r}$ represent the BS-user and relay-user channels for user node i at the k -th sub-carrier, respectively. The channel from BS to the relay and self-interference (SI) channel at the relay utilizing k -th sub-carrier are respectively denoted by $\mathbf{h}_{\text{sr}}^k \in \mathbb{C}^{1 \times N_{\text{BS}}}$ and $\mathbf{h}_{\text{rr}}^k \in \mathbb{C}^{1 \times N_r}$. Moreover we assume all the channels are constant during each frame, frequency-flat in each sub-carrier, and only the imperfect CSI is known. Similar to [24], [25], we consider a CSI error model, where the actual channel can be decomposed into the estimated channel and estimation error, expressed as

$$\begin{aligned} \mathbf{h}_{\mathcal{X}}^k &= \hat{\mathbf{h}}_{\mathcal{X}}^k + \tilde{\mathbf{h}}_{\mathcal{X}}^k, \quad \hat{\mathbf{h}}_{\mathcal{X}}^k \perp \tilde{\mathbf{h}}_{\mathcal{X}}^k, \quad \forall \mathcal{X} \in \{\text{sr}, \text{rr}\}, \forall k \in \mathbb{K}, \\ \mathbf{h}_{\mathcal{Y}}^k &= \hat{\mathbf{h}}_{\mathcal{Y}}^k + \tilde{\mathbf{h}}_{\mathcal{Y}}^k, \quad \hat{\mathbf{h}}_{\mathcal{Y}}^k \perp \tilde{\mathbf{h}}_{\mathcal{Y}}^k, \quad \forall \mathcal{Y} \in \{\text{rd}, \text{sd}\}, \forall k \in \mathbb{K}, \end{aligned} \quad (1)$$

where $\hat{\mathbf{h}}_{\mathcal{X}}^k$ ($\hat{\mathbf{h}}_{\mathcal{Y}}^k$) and $\tilde{\mathbf{h}}_{\mathcal{X}}^k$ ($\tilde{\mathbf{h}}_{\mathcal{Y}}^k$) represent the estimated channel and channel estimation error at the k -th sub-carrier for the relay (user i), respectively. The entries of channel estimation error $\tilde{\mathbf{h}}_{\mathcal{X}}^k$ ($\tilde{\mathbf{h}}_{\mathcal{Y}}^k$) are independent and identically distributed (i.i.d.) complex Gaussian with zero mean and variance $(\sigma_{e,\mathcal{X}}^k)^2$ ($(\sigma_{e,\mathcal{Y}}^k)^2$). We also assume that the estimated channel and the estimation error are uncorrelated³.

B. Signal Model

The transmit signal from the BS is expressed as

$$\mathbf{x}_s^k = \underbrace{\mathbf{v}_{\text{sr}}^k \sqrt{p_{\text{sr},k}}}_{=:\tilde{\mathbf{x}}_s^k} + \sum_{i \in \mathbb{L}} \mathbf{v}_{\text{sd}}^{i,k} \sqrt{p_{\text{sd}}^{i,k}} (s_{\text{sd},k}^i) + \mathbf{e}_{\text{t},s}^k, \quad \forall k \in \mathbb{K}, \quad (2)$$

³The statistical independence can be assumed, for example by considering an MMSE channel estimation strategy [25].

where $\tilde{\mathbf{x}}_s^k$ is the intended transmit signal at the BS. The normalized precoding matrix and transmit power at the BS corresponding to the user i using sub-carrier k are denoted by $\mathbf{v}_{\text{sd}}^{i,k}$ and $p_{\text{sd}}^{i,k}$, respectively. The $s_{\text{sd},k}^i$ represents the unit power transmit symbol for the user i using sub-carrier k , i.e., $\mathbb{E}\{s_{\text{sd},k}^i (s_{\text{sd},k}^i)^*\} = 1$. The transmit distortion at the BS is represented by $\mathbf{e}_{\text{t},s}^k \in \mathbb{C}^{1 \times N_{\text{BS}}}$. Furthermore, the normalized transmit precoding matrix and transmit power at the BS for the relay are denoted by \mathbf{v}_{sr}^k and p_{sr}^k , respectively. The transmit symbol⁴ $s_{\text{sr},k}$ at the BS corresponds to the relay is assumed to be i.i.d with unit power, i.e., $\mathbb{E}\{s_{\text{sr},k} (s_{\text{sr},k})^*\} = 1$.

At the relay, it receives the desired transmit signal from the BS along with the multi-user interference, then decodes the symbols dedicated to each user $\hat{s}_{\text{rd},k}^i$ and then forwards it to the respective users. We assume the retransmitted symbol to be i.i.d. with unit power. The normalized precoding matrix and transmit power at the relay corresponding to the user i utilizing sub-carrier k are denoted by $\mathbf{v}_{\text{rd}}^{i,k}$ and $p_{\text{rd}}^{i,k}$, respectively. Accordingly, the transmit and receive signal at the relay node can be expressed as

$$\begin{aligned} \mathbf{x}_r^k &= \underbrace{\sum_{i \in \mathbb{L}} \mathbf{v}_{\text{rd}}^{i,k} \sqrt{p_{\text{rd}}^{i,k}} s_{\text{rd},k}^i}_{=:\tilde{\mathbf{x}}_r^k} + \mathbf{e}_{\text{t},r}^k, \quad \forall k \in \mathbb{K}, \\ \mathbf{y}_r^k &= \underbrace{\mathbf{h}_{\text{sr}}^k \mathbf{x}_s^k + \mathbf{h}_{\text{rr}}^k \mathbf{x}_r^k}_{=:\tilde{\mathbf{y}}_r^k} + n_r^k + e_{\text{r},r}^k, \quad \forall k \in \mathbb{K}, \end{aligned} \quad (3)$$

where $\mathbf{e}_{\text{t},r}^k \in \mathbb{C}^{N_r \times 1}$, $e_{\text{r},r}^k$ and n_r^k are the transmit distortion, receive distortion and receiver noise at the relay node, respectively. The intended transmit and received signal at the relay can be represented as $\tilde{\mathbf{x}}_r^k$ and $\tilde{\mathbf{y}}_r^k$, respectively. After removing the known part of SI from the received signal by applying SIC, we get

$$\tilde{\mathbf{y}}_r^k = \mathbf{y}_r^k - \hat{\mathbf{h}}_{\text{rr}}^k \tilde{\mathbf{x}}_r^k, \quad \forall k \in \mathbb{K}. \quad (4)$$

Subsequently, the received signal at the user node i can be obtained as

$$\mathbf{y}_d^{i,k} = \underbrace{\mathbf{h}_{\text{sd}}^{i,k} \mathbf{x}_s^k + \mathbf{h}_{\text{rd}}^{i,k} \tilde{\mathbf{x}}_r^k}_{=:\tilde{\mathbf{y}}_d^{i,k}} + n_d^{i,k} + e_{\text{r},d}^{i,k}, \quad \forall k \in \mathbb{K}, \quad (5)$$

where $n_d^{i,k}$, $e_{\text{r},d}^{i,k}$ and $\tilde{\mathbf{y}}_d^{i,k}$ are the receiver noise, receive distortion and intended received signal at the user node i , respectively.

C. Distortion Signal Statistics: The Impact of Limited Dynamic Range

The inaccuracies of hardware components such as analog to digital converter (ADC) and digital to analog converter (DAC) error, noises caused by power amplifiers, automatic gain control (AGC) and oscillator on transmit and receive chains are jointly modelled for FD multiple input multiple output (MIMO) transceiver in [26], [27], based on [28]–[31]. The hardware inaccuracies of the transmit (receive) chain for each antenna is jointly modelled as an additive distortion and can be expressed as

$$\begin{aligned} x_l(t) &= v_l(t) + e_{\text{t},l}(t) \\ y_l(t) &= u_l(t) + e_{\text{r},l}(t), \end{aligned} \quad (6)$$

⁴Please note that the information belonging to all users are combined in the data symbols $s_{\text{sr},k}$, $\forall k$ during the source-relay transmission and separated at the relay, via channel en/decoding. The decoded information belonging to each user is then separately beamformed and transmitted from the relay.

such that,

$$\begin{aligned} e_{t,l}(t) &\sim \mathcal{CN}(0, \kappa_l \mathbb{E}\{|v_l(t)|^2\}), e_{r,l}(t) \sim \mathcal{CN}(0, \beta_l \mathbb{E}\{|u_l(t)|^2\}), \\ e_{t,l}(t) \perp v_l(t), e_{t,l}(t) \perp e_{t,l'}(t), e_{t,l}(t) \perp e_{t,l}(t'), l \neq l', t \neq t' \\ e_{r,l}(t) \perp u_l(t), e_{r,l}(t) \perp e_{r,l'}(t), e_{r,l}(t) \perp e_{r,l}(t'), l \neq l', t \neq t', \end{aligned} \quad (7)$$

i.e., the distortion terms are proportional to the intensity of the intended signals. In the equations (6) and (7), t denotes the instance of time, and v_l (u_l), x_l (y_l), and $e_{t,l}$ ($e_{r,l}$) are respectively the baseband time-domain representation of the intended transmit (receive) signal, the actual transmit (receive) signal, and the additive transmit (receive) distortion at the l -th transmit (receive) chain. The κ_l and β_l are the distortion coefficient for the l -th transmit and receive chain, respectively⁵.

In [22], we have studied the impact of non-linear hardware distortions in the frequency domain specific to an OFDM system. In this work, we extend this characterization for a general orthonormal MC strategy, where the sub-carriers k are orthogonal to each other with a unitary linear transformation, e.g., OVSF-CDMA, OFDM and CP-OFDM. Let \mathbf{Q} be a $K \times K$ unitary transformation matrix, where the columns of the matrix \mathbf{Q} represent the basis of the generalized sub-carrier waveforms which are orthonormal to each other. The total number of sub-carriers is K . NT_s is the duration of one communication block, where T_s is the sample period.

The unitary transformation representation of the sampled time domain signal for each communication block can be written as

$$\begin{aligned} x_l^k &= \sum_{n=0}^{N-1} x_l(nT_s) q_{k,n}^* = \underbrace{\sum_{n=0}^{N-1} v_l(nT_s) q_{k,n}^*}_{=:v_l^k} + \underbrace{\sum_{n=0}^{N-1} e_{t,l}(nT_s) q_{k,n}^*}_{=:e_{t,l}^k} \\ y_l^k &= \sum_{n=0}^{N-1} y_l(nT_s) q_{k,n}^* = \underbrace{\sum_{n=0}^{N-1} u_l(nT_s) q_{k,n}^*}_{=:u_l^k} + \underbrace{\sum_{n=0}^{N-1} e_{r,l}(nT_s) q_{k,n}^*}_{=:e_{r,l}^k} \end{aligned} \quad (8)$$

where $q_{k,n}$ is the element of the unitary matrix \mathbf{Q} at the k -th row and n -th column.

Lemma II.1. *Let us define \tilde{x}_l^m and \tilde{y}_l^m as the intended transmit and receive signal via m -th sub-carrier at the l -th transmit/receive chain. The impact of hardware distortions in the unitary transformed domain is characterized as*

$$e_{t,l}^k \sim \mathcal{CN}\left(0, \frac{\tilde{\kappa}_l}{K} \sum_{m=1}^K \mathbb{E}\{|\tilde{y}_l^m|^2\}\right), e_{t,l}^k \perp \tilde{y}_l^k, e_{t,l}^k \perp e_{t,l'}^k, \quad (9)$$

⁵Please note that in comparison to the widely used receiver thermal noise model for describing the impact of chain inaccuracies, and in contrast to the prior studies on FD multi-carrier systems, the aforementioned characterization includes two additional intuitions. Firstly, it indicates that the variance of the distortion signal is proportional to the transmitted or receiver signal strength. This is in contrast to the traditional thermal noise modeling which assumes an additive noise with a priori known variance. Please note that this is particularly important in controlling the impact of distortions via optimized transmit strategies. Secondly, the distortion signal is temporally and spatially white, i.e., not restricted to a single sub-carrier. The latter indicates that due to the non-linear behavior of hardware distortions, transmission at any sub-carrier will lead to additional distortion level at all sub-carriers, i.e., ICL.

$$e_{r,l}^k \sim \mathcal{CN}\left(0, \frac{\tilde{\beta}_l}{K} \sum_{m=1}^K \mathbb{E}\{|\tilde{x}_l^m|^2\}\right), e_{r,l}^k \perp \tilde{x}_l^k, e_{r,l}^k \perp e_{r,l'}^k, \quad (10)$$

transforming the statistical independence, as well as the proportional variance properties from the time domain. Here, K represents the total number of sub-carriers. $\tilde{\kappa}_l$ and $\tilde{\beta}_l$ correspond to the transmit and receive distortion coefficient at the l -th transmit/receive chain.

Proof: Please refer to the Appendix. \blacksquare

The statistics of the distortion terms can be obtained using Lemma II.1,

$$e_{t,s}^k \sim \mathcal{CN}\left(\mathbf{0}_{N_{\text{BS}}}, \frac{1}{K} \tilde{\Theta}_{t,s} \sum_{k \in \mathbb{K}} \text{diag}\left(\mathbb{E}\{\tilde{\mathbf{x}}_s^k (\tilde{\mathbf{x}}_s^k)^H\}\right)\right), \quad (11)$$

$$e_{t,r}^k \sim \mathcal{CN}\left(\mathbf{0}_{N_r}, \frac{1}{K} \tilde{\Theta}_{t,r} \sum_{k \in \mathbb{K}} \text{diag}\left(\mathbb{E}\{\tilde{\mathbf{x}}_r^k (\tilde{\mathbf{x}}_r^k)^H\}\right)\right), \quad (12)$$

$$e_{r,r}^k \sim \mathcal{CN}\left(0, \frac{\tilde{\beta}_r}{K} \sum_{k \in \mathbb{K}} \left(\mathbb{E}\{\tilde{\mathbf{y}}_r^k (\tilde{\mathbf{y}}_r^k)^H\}\right)\right), \quad (13)$$

$$e_{r,d}^{i,k} \sim \mathcal{CN}\left(0, \frac{\tilde{\beta}_d^i}{K} \sum_{k \in \mathbb{K}} \left(\mathbb{E}\{\tilde{\mathbf{y}}_d^{i,k} (\tilde{\mathbf{y}}_d^{i,k})^H\}\right)\right), \quad (14)$$

where diagonal matrix $\tilde{\Theta}_{t,r}$ ($\tilde{\Theta}_{t,s}$) consists of transmit distortion coefficients for the corresponding chains at the relay (BS). $\tilde{\beta}_r$ ($\tilde{\beta}_d^i$) represents the receive distortion coefficient at the relay (user i).

D. Achievable Rate

For further calculations, let us define $\beta_d^i = \frac{\tilde{\beta}_d^i}{K}$, $\beta_r = \frac{\tilde{\beta}_r}{K}$, $\Theta_{t,s} = \frac{1}{K} \tilde{\Theta}_{t,s}$ and $\Theta_{t,r} = \frac{1}{K} \tilde{\Theta}_{t,r}$. The received collective interference-plus-distortion-plus-noise variance at the relay can be formulated as in (15). The approximation (15) is obtained considering $\tilde{\kappa}_l, \tilde{\beta}_l \ll 1$ and hence the terms including higher orders of the distortion coefficients can be ignored. Please note that (15) holds as all components of thermal noise, transmit and receive distortions, and the transmitted data symbols are all zero-mean and mutually independent.

At the user end, the received signal is processed in two phases using successive interference cancellation technique. In the first phase, the received signal from the BS is considered as interference while considering the strong received signal from the relay as desired signal. In the second phase, as the received from the relay is already known, it can be removed from the received signal which in turn reduces the total interference. The covariance of received collective interference-plus-noise signal at the user for the first phase can be expressed as in (16). Similar to (15), (16) is obtained considering $\tilde{\kappa}_l, \tilde{\beta}_l \ll 1$ as well as the independence of the various signal components. At the second phase, the signal from the relay is known and it can be removed from the received signal⁶, whereas the signal from the BS to user will be treated as the desired signal. The covariance of received collective interference-plus-noise signal at the user for the second phase can be hence obtained as

⁶At the second stage of SuIC, only the desired signal part of the relay signal can be removed. However, the residual interference from the relay signal remains while decoding the BS signal at the user.

$$\begin{aligned}
\Sigma_r^k &\approx \underbrace{\sum_{j \in \mathbb{L}} \widehat{\mathbf{h}}_{\text{sr}}^k \mathbf{v}_{\text{sd}}^{j,k} p_{\text{sd}}^{j,k} (\mathbf{v}_{\text{sd}}^{j,k})^H (\widehat{\mathbf{h}}_{\text{sr}}^k)^H}_{\text{Co-channel interference}} + \underbrace{(\sigma_{\text{e, sr}}^k)^2 (p_{\text{sr}}^k + \sum_{j \in \mathbb{L}} p_{\text{sd}}^{j,k})}_{\text{Relay SI channel estimation error}} + \underbrace{(\sigma_{\text{e, rr}}^k)^2 \sum_{j \in \mathbb{L}} p_{\text{rd}}^{j,k}}_{\text{Thermal noise}} + \underbrace{(\sigma_{\text{n, r}}^k)^2}_{\text{Thermal noise}} \\
&+ \beta_r \underbrace{\sum_{m \in \mathbb{K}} \left(\widehat{\mathbf{h}}_{\text{sr}}^m (\mathbf{v}_{\text{sr}}^m p_{\text{sr}}^m (\mathbf{v}_{\text{sr}}^m)^H + \sum_{j \in \mathbb{L}} \mathbf{v}_{\text{sd}}^{j,m} p_{\text{sd}}^{j,m} (\mathbf{v}_{\text{sd}}^{j,m})^H) (\widehat{\mathbf{h}}_{\text{sr}}^m)^H + (\sigma_{\text{e, sr}}^m)^2 (p_{\text{sr}}^m + \sum_{j \in \mathbb{L}} p_{\text{sd}}^{j,m}) + \sum_{j \in \mathbb{L}} \widehat{\mathbf{h}}_{\text{rr}}^m \mathbf{v}_{\text{rd}}^{j,m} p_{\text{rd}}^{j,m} (\mathbf{v}_{\text{rd}}^{j,m})^H (\widehat{\mathbf{h}}_{\text{rr}}^m)^H + \sum_{j \in \mathbb{L}} (\sigma_{\text{e, rr}}^m)^2 p_{\text{rd}}^{j,m} + (\sigma_{\text{n, r}}^m)^2 \right)}_{\text{Relay receive distortion}} \\
&+ \underbrace{\widehat{\mathbf{h}}_{\text{sr}}^k \Theta_{\text{t, s}} \sum_{m \in \mathbb{K}} \left(\text{diag} \left(\mathbf{v}_{\text{sr}}^m p_{\text{sr}}^m (\mathbf{v}_{\text{sr}}^m)^H \right) + \sum_{j \in \mathbb{L}} \text{diag} \left(\mathbf{v}_{\text{sd}}^{j,m} p_{\text{sd}}^{j,m} (\mathbf{v}_{\text{sd}}^{j,m})^H \right) \right) (\widehat{\mathbf{h}}_{\text{sr}}^k)^H + (\sigma_{\text{e, sr}}^k)^2 \text{Tr} \left(\Theta_{\text{t, s}} \sum_{m \in \mathbb{K}} \left(\text{diag} \left(\mathbf{v}_{\text{sr}}^m p_{\text{sr}}^m (\mathbf{v}_{\text{sr}}^m)^H \right) + \sum_{j \in \mathbb{L}} \text{diag} \left(\mathbf{v}_{\text{sd}}^{j,m} p_{\text{sd}}^{j,m} (\mathbf{v}_{\text{sd}}^{j,m})^H \right) \right) \right)}_{\text{BS transmit distortion}} \\
&+ \underbrace{\widehat{\mathbf{h}}_{\text{rr}}^k \Theta_{\text{t, r}} \sum_{j \in \mathbb{L}} \sum_{m \in \mathbb{K}} \text{diag} \left(\mathbf{v}_{\text{rd}}^{j,m} p_{\text{rd}}^{j,m} (\mathbf{v}_{\text{rd}}^{j,m})^H \right) (\widehat{\mathbf{h}}_{\text{rr}}^k)^H + (\sigma_{\text{e, rr}}^k)^2 \sum_{j \in \mathbb{L}} \sum_{m \in \mathbb{K}} \text{Tr} \left(\Theta_{\text{t, r}} \text{diag} \left(\mathbf{v}_{\text{rd}}^{j,m} p_{\text{rd}}^{j,m} (\mathbf{v}_{\text{rd}}^{j,m})^H \right) \right)}_{\text{Relay transmit distortion}}, \quad \forall k \in \mathbb{K},
\end{aligned} \tag{15}$$

$$\begin{aligned}
\Sigma_{\text{d},1}^{i,k} &\approx \underbrace{\widehat{\mathbf{h}}_{\text{sd}}^{i,k} \left(\mathbf{v}_{\text{sr}}^{k,k} p_{\text{sr}}^k (\mathbf{v}_{\text{sr}}^k)^H + \sum_{j \in \mathbb{L}} \mathbf{v}_{\text{sd}}^{j,k} p_{\text{sd}}^{j,k} (\mathbf{v}_{\text{sd}}^{j,k})^H \right) (\widehat{\mathbf{h}}_{\text{sd}}^{i,k})^H + (\sigma_{\text{e, sd}}^{i,k})^2 (p_{\text{sr}}^k + \sum_{j \in \mathbb{L}} p_{\text{sd}}^{j,k}) + \sum_{j \in \mathbb{L}, i \neq j} \widehat{\mathbf{h}}_{\text{rd}}^{i,k} \mathbf{v}_{\text{rd}}^{j,k} p_{\text{rd}}^{j,k} (\mathbf{v}_{\text{rd}}^{j,k})^H (\widehat{\mathbf{h}}_{\text{rd}}^{i,k})^H + (\sigma_{\text{e, rd}}^{i,k})^2 \sum_{j \in \mathbb{L}} p_{\text{rd}}^{j,k} + (\sigma_{\text{n, d}}^{i,k})^2}_{\text{Co-channel interference}} \\
&+ \underbrace{\widehat{\mathbf{h}}_{\text{sd}}^{i,k} \Theta_{\text{t, s}} \sum_{m \in \mathbb{K}} \left(\text{diag} \left(\mathbf{v}_{\text{sr}}^m p_{\text{sr}}^m (\mathbf{v}_{\text{sr}}^m)^H \right) + \sum_{j \in \mathbb{L}} \text{diag} \left(\mathbf{v}_{\text{sd}}^{j,m} p_{\text{sd}}^{j,m} (\mathbf{v}_{\text{sd}}^{j,m})^H \right) \right) (\widehat{\mathbf{h}}_{\text{sd}}^{i,k})^H + (\sigma_{\text{e, sd}}^{i,k})^2 \text{Tr} \left(\Theta_{\text{t, s}} \sum_{m \in \mathbb{K}} \left(\text{diag} \left(\mathbf{v}_{\text{sr}}^m p_{\text{sr}}^m (\mathbf{v}_{\text{sr}}^m)^H \right) + \sum_{j \in \mathbb{L}} \text{diag} \left(\mathbf{v}_{\text{sd}}^{j,m} p_{\text{sd}}^{j,m} (\mathbf{v}_{\text{sd}}^{j,m})^H \right) \right) \right)}_{\text{BS transmit distortion}} \\
&+ \underbrace{\beta_d \sum_{m \in \mathbb{K}} \left(\widehat{\mathbf{h}}_{\text{sr}}^{i,m} (\mathbf{v}_{\text{sr}}^m p_{\text{sr}}^m (\mathbf{v}_{\text{sr}}^m)^H + \sum_{j \in \mathbb{L}} \mathbf{v}_{\text{sd}}^{j,m} p_{\text{sd}}^{j,m} (\mathbf{v}_{\text{sd}}^{j,m})^H) (\widehat{\mathbf{h}}_{\text{sr}}^{i,m})^H + (\sigma_{\text{e, sd}}^{i,m})^2 (p_{\text{sr}}^m + \sum_{j \in \mathbb{L}} p_{\text{sd}}^{j,m}) + \sum_{j \in \mathbb{L}} \left(\widehat{\mathbf{h}}_{\text{rd}}^{i,m} \mathbf{v}_{\text{rd}}^{j,m} p_{\text{rd}}^{j,m} (\mathbf{v}_{\text{rd}}^{j,m})^H (\widehat{\mathbf{h}}_{\text{rd}}^{i,m})^H + (\sigma_{\text{e, rd}}^{i,m})^2 p_{\text{rd}}^{j,m} \right) + (\sigma_{\text{n, d}}^{i,m})^2 \right)}_{\text{User receive distortion}} \\
&+ \underbrace{\sum_{j \in \mathbb{L}} \sum_{m \in \mathbb{K}} \left(\widehat{\mathbf{h}}_{\text{rd}}^{i,k} \Theta_{\text{t, r}} \text{diag} \left(\mathbf{v}_{\text{rd}}^{j,m} p_{\text{rd}}^{j,m} (\mathbf{v}_{\text{rd}}^{j,m})^H \right) (\widehat{\mathbf{h}}_{\text{rd}}^{i,k})^H + (\sigma_{\text{e, rd}}^{i,k})^2 \text{Tr} \left(\Theta_{\text{t, r}} \text{diag} \left(\mathbf{v}_{\text{rd}}^{j,m} p_{\text{rd}}^{j,m} (\mathbf{v}_{\text{rd}}^{j,m})^H \right) \right) \right)}_{\text{Relay transmit distortion}}, \quad \forall k \in \mathbb{K}, \quad \forall i \in \mathbb{L},
\end{aligned} \tag{16}$$

$$\Sigma_{\text{d},2}^{i,k} := \Sigma_{\text{d},1}^{i,k} - \widehat{\mathbf{h}}_{\text{sd}}^{i,k} \left(\mathbf{v}_{\text{sd}}^{i,k} p_{\text{sd}}^{i,k} (\mathbf{v}_{\text{sd}}^{i,k})^H \right) (\widehat{\mathbf{h}}_{\text{sd}}^{i,k})^H. \tag{17}$$

By assuming a Gaussian distribution for the desired signal, distortion and interference components, as well as a sufficiently large coding block length⁷, the achievable information rate for the BS to relay link at the sub-carrier k is expressed as

$$R_{\text{sr}}^k = \gamma_0 \log_2 \left(1 + \frac{|\widehat{\mathbf{h}}_{\text{sr}}^k \mathbf{v}_{\text{sr}}^k|^2 p_{\text{sr}}^k}{\alpha_r^k + \sum_{m \in \mathbb{K}} \left(\gamma_{\text{sr}}^{km} p_{\text{sr}}^m + \sum_{j \in \mathbb{L}} \left(\gamma_{\text{rd},j}^{km} p_{\text{rd}}^{j,m} + \gamma_{\text{sd},j}^{km} p_{\text{sd}}^{j,m} \right) \right) \right), \tag{18}$$

where $\gamma_0 = (T_{\text{tot}} - T_{\text{train}})/T_{\text{tot}}$ represents the fraction of time interval allocated for the data transmission. The channel coherence time interval and channel estimation (training) time interval are denoted by T_{tot} and T_{train} , respectively. And

$$\begin{aligned}
\gamma_{\text{sr}}^{km} &= \delta_{km} (\sigma_{\text{e, sr}}^m)^2 + \widehat{\mathbf{h}}_{\text{sr}}^k \Theta_{\text{t, s}} \text{diag} \left(\mathbf{v}_{\text{sr}}^m (\mathbf{v}_{\text{sr}}^m)^H \right) (\widehat{\mathbf{h}}_{\text{sr}}^k)^H \\
&+ (\sigma_{\text{e, sr}}^k)^2 \text{Tr} \left(\Theta_{\text{t, s}} \text{diag} \left(\mathbf{v}_{\text{sr}}^m (\mathbf{v}_{\text{sr}}^m)^H \right) \right)
\end{aligned}$$

$$\begin{aligned}
&+ \beta_r \left(\widehat{\mathbf{h}}_{\text{sr}}^m \mathbf{v}_{\text{sr}}^m p_{\text{sr}}^m (\mathbf{v}_{\text{sr}}^m)^H (\widehat{\mathbf{h}}_{\text{sr}}^m)^H + (\sigma_{\text{e, sr}}^m)^2 \right), \\
\gamma_{\text{rd},j}^{km} &= \delta_{km} (\sigma_{\text{e, rr}}^m)^2 + \widehat{\mathbf{h}}_{\text{rr}}^k \Theta_{\text{t, r}} \text{diag} \left(\mathbf{v}_{\text{rd}}^{j,m} (\mathbf{v}_{\text{rd}}^{j,m})^H \right) (\widehat{\mathbf{h}}_{\text{rr}}^k)^H \\
&+ (\sigma_{\text{e, rr}}^k)^2 \text{Tr} \left(\Theta_{\text{t, r}} \text{diag} \left(\mathbf{v}_{\text{rd}}^{j,m} (\mathbf{v}_{\text{rd}}^{j,m})^H \right) \right) \\
&+ \beta_r \left(\widehat{\mathbf{h}}_{\text{rr}}^k \mathbf{v}_{\text{rd}}^{j,m} p_{\text{rd}}^{j,m} (\mathbf{v}_{\text{rd}}^{j,m})^H (\widehat{\mathbf{h}}_{\text{rr}}^k)^H + (\sigma_{\text{e, rr}}^m)^2 \right), \\
\gamma_{\text{sd},j}^{km} &= \delta_{km} \left(\widehat{\mathbf{h}}_{\text{sr}}^m \mathbf{v}_{\text{sd}}^{j,m} p_{\text{sd}}^{j,m} (\mathbf{v}_{\text{sd}}^{j,m})^H (\widehat{\mathbf{h}}_{\text{sr}}^m)^H + (\sigma_{\text{e, sr}}^m)^2 \right) \\
&+ \widehat{\mathbf{h}}_{\text{sr}}^k \Theta_{\text{t, s}} \text{diag} \left(\mathbf{v}_{\text{sd}}^{j,m} (\mathbf{v}_{\text{sd}}^{j,m})^H \right) (\widehat{\mathbf{h}}_{\text{sr}}^k)^H \\
&+ (\sigma_{\text{e, sr}}^k)^2 \text{Tr} \left(\Theta_{\text{t, s}} \text{diag} \left(\mathbf{v}_{\text{sd}}^{j,m} (\mathbf{v}_{\text{sd}}^{j,m})^H \right) \right) \\
&+ \beta_r \left(\widehat{\mathbf{h}}_{\text{sr}}^m \mathbf{v}_{\text{sd}}^{j,m} p_{\text{sd}}^{j,m} (\mathbf{v}_{\text{sd}}^{j,m})^H (\widehat{\mathbf{h}}_{\text{sr}}^m)^H + (\sigma_{\text{e, sr}}^m)^2 \right), \\
\alpha_r^k &= (\sigma_{\text{n, r}}^k)^2 + \beta_r \sum_{m \in \mathbb{K}} (\sigma_{\text{n, r}}^m)^2, \tag{19}
\end{aligned}$$

such that the coefficients $\{\gamma_{\text{sd},j}^{km}\}, \{\gamma_{\text{sr}}^{km}\}, \{\gamma_{\text{rd},j}^{km}\}$ represent the impacts of inter-carrier leakage when $m \neq k$. Similarly, the achievable information rate for the link between the relay to the user i , using sub-carrier k is expressed as

⁷Please note that in this work, we consider the scenario where the statistics of CSI error as well as the hardware impairments can be obtained, relying on the reported experimental characterizations of hardware impairments and CSI error. Moreover, the employed rate expressions are valid assuming a Gaussian distribution for all signals and a sufficiently long coding block. When the aforementioned assumptions are not accurate, the subsequent analysis should be viewed as an approximation.

$$R_{rd}^{i,k} = \gamma_0 \log_2 \left(1 + \frac{|\hat{\mathbf{h}}_{rd}^{i,k} \mathbf{v}_{rd}^{i,k}|^2 p_{rd}^{i,k}}{\alpha_d^{i,k} + \sum_{m \in \mathbb{K}} \left(\bar{\gamma}_{sr,i}^{km} p_{sr}^m + \sum_{j \in \mathbb{L}} \left(\bar{\gamma}_{rd,ij}^{km} p_{rd}^{j,m} + \bar{\gamma}_{sd,ij}^{km} p_{sd}^{j,m} \right) \right)} \right) \quad (20)$$

where

$$\begin{aligned} \bar{\gamma}_{sr,i}^{km} &= \delta_{km} \left(\hat{\mathbf{h}}_{sd}^{i,m} \mathbf{v}_{sr}^m (\mathbf{v}_{sr}^m)^H (\hat{\mathbf{h}}_{sd}^{i,m})^H + (\sigma_{e,rd}^{i,m})^2 \right) \\ &\quad + \hat{\mathbf{h}}_{sd}^{i,k} \mathbf{\Theta}_{t,s} \text{diag} \left(\mathbf{v}_{sr}^m (\mathbf{v}_{sr}^m)^H \right) (\hat{\mathbf{h}}_{sd}^{i,k})^H \\ &\quad + (\sigma_{e,rd}^{i,k})^2 \text{Tr} \left(\mathbf{\Theta}_{t,s} \text{diag} \left(\mathbf{v}_{sr}^m (\mathbf{v}_{sr}^m)^H \right) \right) \\ &\quad + \beta_d^i \left(\hat{\mathbf{h}}_{sd}^{i,m} \mathbf{v}_{sr}^m (\mathbf{v}_{sr}^m)^H (\hat{\mathbf{h}}_{sd}^{i,m})^H + (\sigma_{e,rd}^{i,m})^2 \right), \\ \bar{\gamma}_{rd,ij}^{km} &= \delta_{km} (1 - \delta_{ij}) \hat{\mathbf{h}}_{rd}^{i,k} \mathbf{v}_{rd}^{j,m} (\mathbf{v}_{rd}^{j,m})^H (\hat{\mathbf{h}}_{rd}^{i,k})^H + \delta_{km} (\sigma_{e,rd}^{i,m})^2 \\ &\quad + \hat{\mathbf{h}}_{rd}^{i,k} \mathbf{\Theta}_{t,r} \text{diag} \left(\mathbf{v}_{rd}^{j,m} (\mathbf{v}_{rd}^{j,m})^H \right) (\hat{\mathbf{h}}_{rd}^{i,k})^H \\ &\quad + (\sigma_{e,rd}^{i,k})^2 \text{Tr} \left(\mathbf{\Theta}_{t,r} \text{diag} \left(\mathbf{v}_{rd}^{j,m} (\mathbf{v}_{rd}^{j,m})^H \right) \right) \\ &\quad + \beta_d^i \left(\hat{\mathbf{h}}_{rd}^{i,m} \mathbf{v}_{rd}^{j,m} (\mathbf{v}_{rd}^{j,m})^H (\hat{\mathbf{h}}_{rd}^{i,m})^H + (\sigma_{e,rd}^{i,m})^2 \right), \\ \bar{\gamma}_{sd,ij}^{km} &= \delta_{km} \left(\hat{\mathbf{h}}_{sd}^{i,m} \mathbf{v}_{sd}^{j,m} (\mathbf{v}_{sd}^{j,m})^H (\hat{\mathbf{h}}_{sd}^{i,m})^H + (\sigma_{e,rd}^{i,m})^2 \right) \\ &\quad + \hat{\mathbf{h}}_{sd}^{i,k} \mathbf{\Theta}_{t,s} \text{diag} \left(\mathbf{v}_{sd}^{j,m} (\mathbf{v}_{sd}^{j,m})^H \right) (\hat{\mathbf{h}}_{sd}^{i,k})^H \\ &\quad + (\sigma_{e,rd}^{i,k})^2 \text{Tr} \left(\mathbf{\Theta}_{t,s} \text{diag} \left(\mathbf{v}_{sd}^{j,m} (\mathbf{v}_{sd}^{j,m})^H \right) \right) \\ &\quad + \beta_d^i \left(\hat{\mathbf{h}}_{sd}^{i,m} \mathbf{v}_{sd}^{j,m} (\mathbf{v}_{sd}^{j,m})^H (\hat{\mathbf{h}}_{sd}^{i,m})^H + (\sigma_{e,rd}^{i,m})^2 \right), \\ \alpha_d^{i,k} &= (\sigma_{n,d}^{i,k})^2 + \beta_d^i \sum_{m \in \mathbb{K}} (\sigma_{n,d}^{i,m})^2, \end{aligned} \quad (21)$$

such that the coefficients $\{\bar{\gamma}_{sd,ij}^{km}\}$, $\{\bar{\gamma}_{sr,i}^{km}\}$, $\{\bar{\gamma}_{rd,ij}^{km}\}$ represent the impacts of inter-user interference, when $i \neq j$, and the impact of inter-carrier leakage when $m \neq k$. Subsequently, the achievable information rate between the BS and user i , using sub-carrier k can be expressed as

$$R_{sd}^{i,k} = \gamma_0 \log_2 \left(1 + \frac{|\hat{\mathbf{h}}_{sd}^{i,k} \mathbf{v}_{sd}^{i,k}|^2 p_{sd}^{i,k}}{\alpha_d^{i,k} + \sum_{m \in \mathbb{K}} \left(\bar{\gamma}_{sr,i}^{km} p_{sr}^m + \sum_{j \in \mathbb{L}} \left(\bar{\gamma}_{rd,ij}^{km} p_{rd}^{j,m} + \bar{\gamma}_{sd,ij}^{km} p_{sd}^{j,m} \right) \right)} \right) \quad (22)$$

where

$$\bar{\gamma}_{sd,ij}^{km} = \bar{\gamma}_{sd,ij}^{km} - \delta_{km} \delta_{ij} \left(\hat{\mathbf{h}}_{sd}^{i,m} \mathbf{v}_{sd}^{j,m} (\mathbf{v}_{sd}^{j,m})^H (\hat{\mathbf{h}}_{sd}^{i,m})^H \right). \quad (23)$$

Please note that although the FD relay is capable of concurrent reception and transmission, compared to the direct link, the additional decoding latency at the relay will lead to a larger overall coding latency for the information transmitted via the relay link. Nevertheless, the direct link will experience a larger processing latency, since the information from the relay link needs to be first decoded and subtracted. The total achievable downlink information rate, combining the downlink information transmitted for all users and at all sub-carriers can hence be written as

$$R_{\text{sum}} = \sum_{k \in \mathbb{K}} \sum_{i \in \mathbb{L}} R_{sd}^{i,k} + \min \left\{ \sum_{k \in \mathbb{K}} R_{sr}^k, \sum_{k \in \mathbb{K}} \sum_{i \in \mathbb{L}} R_{rd}^{i,k} \right\}. \quad (24)$$

III. JOINT POWER AND SUB-CARRIER ALLOCATION FOR THE SUIC ENABLED NETWORK

In this section, we present the joint sub-carrier and power allocation optimization problem for the studied system, to maximize spectral efficiency in terms of total sum-rate under transmit power constraints. Please note that the studied power optimization problem also subsumes the problem of optimal sub-carrier allocation, such that if the power allocated to the node for a particular sub-carrier is zero, then the node is not transmitting or receiving in that particular sub-carrier. The sum-rate maximization problem for the multi-user case can be formulated as

$$\begin{aligned} &\text{maximize} && R_{\text{sum}} \\ &p_{sd}^{i,k} \geq 0, p_{sr}^k \geq 0, \\ &p_{rd}^{i,k} \geq 0 \\ &\text{subject to} && \sum_{i \in \mathbb{L}} \sum_{k \in \mathbb{K}} p_{rd}^{i,k} \leq P_r, \quad \sum_{i \in \mathbb{L}} \sum_{k \in \mathbb{K}} p_{sd}^{i,k} + \sum_{k \in \mathbb{K}} p_{sr}^k \leq P_s, \end{aligned} \quad (25)$$

where P_s and P_r are the available transmit power at the BS and the relay, respectively. Please note that the above problem is a non-convex and non-smooth optimization problem, due to the non-linear objective expressed in (24). Our goal is to implement an iterative optimization problem where in each iteration a convex sub-problem is solved. In order to simplify the structure presented in (25), by employing the equivalent epigraph presentation for the rate associated with the relay link, the problem (25) is equivalently reformulated as

$$\begin{aligned} &\text{maximize} && \sum_{i \in \mathbb{L}} \sum_{k \in \mathbb{K}} R_{sd}^{i,k} + t \\ &p_{sd}^{i,k} \geq 0, p_{sr}^k \geq 0, t \\ &p_{rd}^{i,k} \geq 0 \\ &\text{subject to} && \sum_{k \in \mathbb{K}} R_{sr}^k \geq t, \quad \sum_{i \in \mathbb{L}} \sum_{k \in \mathbb{K}} R_{rd}^{i,k} \geq t, \\ &&& \sum_{i \in \mathbb{L}} \sum_{k \in \mathbb{K}} p_{rd}^{i,k} \leq P_r, \quad \sum_{i \in \mathbb{L}} \sum_{k \in \mathbb{K}} p_{sd}^{i,k} + \sum_{k \in \mathbb{K}} p_{sr}^k \leq P_s. \end{aligned} \quad (26)$$

where t is introduced as an auxiliary variable, transferring parts of the problem objective in (25) into the constraint set in (26). Please note that the problem (26) is still a non-convex optimization problem. Nevertheless, it is a smooth problem belonging to the class of DC optimization problems, which is solved using an iterative algorithm via the SIA framework, with a necessary convergence to a point satisfying KKT optimality conditions [23]. By employing the Taylor's approximation on the concave terms, a lower bound on the rate expression R_{sr}^k is obtained as in (27), where $p_{rd,0}^k, p_{sd,0}^k$ and $p_{sr,0}^k$ are the fixed points of the Taylor's approximation. Undertaking a similar procedure, the lower bound of $R_{sd}^{i,k}$ and $R_{rd}^{i,k}$ are obtained as $\bar{R}_{sd}^{i,k}$ and $\bar{R}_{rd}^{i,k}$. By replacing the actual rate functions with the obtained lower bounds, the optimization problem (25) is approximated as

$$\begin{aligned} &\text{maximize} && \sum_{i \in \mathbb{L}} \sum_{k \in \mathbb{K}} \bar{R}_{sd}^{i,k} + t \\ &p_{sd}^{i,k} \geq 0, p_{sr}^k \geq 0, \\ &p_{rd}^{i,k} \geq 0, t \\ &\text{subject to} && \sum_{k \in \mathbb{K}} \bar{R}_{sr}^k \geq t, \quad \sum_{i \in \mathbb{L}} \sum_{k \in \mathbb{K}} \bar{R}_{rd}^{i,k} \geq t, \\ &&& \sum_{i \in \mathbb{L}} \sum_{k \in \mathbb{K}} p_{rd}^{i,k} \leq P_r, \quad \sum_{i \in \mathbb{L}} \sum_{k \in \mathbb{K}} p_{sd}^{i,k} + \sum_{k \in \mathbb{K}} p_{sr}^k \leq P_s. \end{aligned} \quad (28)$$

$$\begin{aligned}
R_{\text{sr}}^k &\geq \gamma_0 \log_2 \left(|\hat{\mathbf{h}}_{\text{sr}}^k \mathbf{v}_{\text{sr}}^k|^2 p_{\text{sr}}^k + \alpha_r^k + \sum_{m \in \mathbb{K}} \left(\gamma_{\text{sr}}^{km} p_{\text{sr}}^m + \sum_{j \in \mathbb{L}} \left(\gamma_{\text{rd},j}^{km} p_{\text{rd}}^{j,m} + \gamma_{\text{sd},j}^{km} p_{\text{sd}}^{j,m} \right) \right) \right) - \gamma_0 \log_2 \left(\alpha_r^k + \sum_{m \in \mathbb{K}} \left(\gamma_{\text{sr}}^{km} p_{\text{sr},0}^m + \sum_{j \in \mathbb{L}} \left(\gamma_{\text{rd},j}^{km} p_{\text{rd},0}^{j,m} + \gamma_{\text{sd},j}^{km} p_{\text{sd},0}^{j,m} \right) \right) \right) \\
&- \frac{\gamma_0 \sum_{m \in \mathbb{K}} \left(\gamma_{\text{sr}}^{km} \left(p_{\text{sr}}^m - p_{\text{sr},0}^m \right) + \sum_{j \in \mathbb{L}} \left(\gamma_{\text{rd},j}^{km} \left(p_{\text{rd}}^{j,m} - p_{\text{rd},0}^{j,m} \right) + \gamma_{\text{sd},j}^{km} \left(p_{\text{sd}}^{j,m} - p_{\text{sd},0}^{j,m} \right) \right) \right)}{\log(2) \left(\alpha_r^k + \sum_{m \in \mathbb{K}} \left(\gamma_{\text{sr}}^{km} p_{\text{sr},0}^m + \sum_{j \in \mathbb{L}} \left(\gamma_{\text{rd},j}^{km} p_{\text{rd},0}^{j,m} + \gamma_{\text{sd},j}^{km} p_{\text{sd},0}^{j,m} \right) \right) \right)} =: \bar{R}_{\text{sr}}^k.
\end{aligned} \tag{27}$$

The above optimization is a jointly convex problem and hence can be solved to optimality via a standard convex solver [32]. This enables an iterative update of the optimization variables, where at each iteration the approximated rate functions are updated with the solution of (28) from the previous iteration as their initial points. The iterative update leads to a monotonic increment of the objective and is continued until a stable point is reached. Please note that due to the application of the first-order Taylor's approximation on the smooth convex terms, the approximation⁸ \bar{R}_{sr}^k is, firstly, a global lower bound to the rate function R_{sr}^k , and secondly, is tight and shares the same slope with R_{sr}^k at the point of approximation, i.e., $p_{\text{rd},0}^k, p_{\text{sd},0}^k, p_{\text{sr},0}^k$. As a result, it complies with the conditions stated in [23, Theorem 1] and enjoys convergence to a KKT solution. Algorithm 1 provides the detailed procedure.

Algorithm 1 Sum-rate maximization

- 1: $a \leftarrow 0$ (set iteration number to zero)
 - 2: $p_{\text{rd},0}^{i,k}, p_{\text{sd},0}^{i,k}, p_{\text{sr},0}^k \leftarrow$ feasible initialization
 - 3: **repeat**
 - 4: $a \leftarrow a + 1$
 - 5: $p_{\text{rd}}^{i,k}, p_{\text{sd}}^{i,k}, p_{\text{sr}}^k \leftarrow$ solve (28)
 - 6: $(p_{\text{rd},0}^{i,k}, p_{\text{sd},0}^{i,k}, p_{\text{sr},0}^k) \leftarrow (p_{\text{rd}}^{i,k}, p_{\text{sd}}^{i,k}, p_{\text{sr}}^k)$,
 - 7: **until** a stable point, or maximum number of a reached
 - 8: **return** $\{p_{\text{rd}}^{i,k}, p_{\text{sd}}^{i,k}, p_{\text{sr}}^k\}$
-

IV. ENABLING DUC VIA HALF DUPLEX RELAY

In this section, we derive the optimization problem in terms of sum-rate maximization for our system, where the relay is an HD relay, and the receiver is capable of performing SuIC, so that DuC can be established. Unlike the FD relay, which can receive and transmit at the same frequency-time channel, the HD relay has to listen to the BS at the first time slot and then forwards the signals to the users in the second time slot. The user receives signals from the BS in both time slots. Hence the SuIC is applicable only in the second time slot, where the user receives signals from both the relay and the BS simultaneously. Moreover, in the first time slot, the BS transmit the signals to the relay and the user. Since the relay is operated in HD, there is no SI at the relay. We also assume the channel remains the same throughout the entire communication (both the time slots).

During the first time slot, the BS transmits the signal to the users as well as the relay. There is no communication between the relay and user nodes. Therefore, there is no SI at the relay.

The transmit signal from the BS during the first time slot can be expressed as

$$\mathbf{x}_{\text{s,HD1}}^k = \underbrace{\mathbf{v}_{\text{sr}}^k \sqrt{p_{\text{sr},1}^k} s_r^k + \sum_{i \in \mathbb{L}} \mathbf{v}_{\text{sd},1}^{i,k} \sqrt{p_{\text{sd},1}^{i,k}} s_{\text{sd},1}^{i,k}}_{:=\tilde{\mathbf{x}}_{\text{s,HD1}}^k} + \mathbf{e}_{\text{t,s},1}^k, \quad \forall k \in \mathbb{K}, \tag{29}$$

where $\tilde{\mathbf{x}}_{\text{s,HD1}}^k$ is the intended transmit signal at the BS during the first time slot. For the first time slot, the normalized precoding matrix and transmit power corresponding to the user i using sub-carrier k are denoted by $\mathbf{v}_{\text{sd},1}^{i,k}$ and $p_{\text{sd},1}^{i,k}$, respectively. Unit power transmit symbols s_r^k and $s_{\text{sd},1}^{i,k}$ corresponds to the relay link and direct link, respectively. The received signal at the relay and user i can be formulated as

$$\begin{aligned}
\bar{y}_{\text{r,HD1}}^k &= \underbrace{\mathbf{h}_{\text{sr}}^k \mathbf{x}_{\text{s,HD1}}^k + n_r^k}_{:=\tilde{y}_{\text{r,HD1}}^k} + e_{\text{r,r}}^k, \\
y_{\text{d},1}^{i,k} &= \underbrace{\mathbf{h}_{\text{sd}}^{i,k} \mathbf{x}_{\text{s,HD1}}^k + n_{\text{d}}^{i,k}}_{:=\tilde{y}_{\text{d},1}^{i,k}} + e_{\text{r,d},1}^{i,k}, \quad \forall k \in \mathbb{K}.
\end{aligned} \tag{30}$$

Subsequently, during the second time slot, the user receives signals from both the relay and the BS simultaneously and uses SuIC technique to decode both the signals. Similarly, as the previous FD relay case, we assume the relay link between the relay and user nodes are stronger compared to the direct link between the BS and the user nodes. Therefore, the user node first decodes the relay link considering the direct link as noise, and then removes the signal of the relay link from the received signal and decodes the signal from the direct link.

The transmit signal at the BS and the relay during second time slot can be written as

$$\begin{aligned}
\mathbf{x}_{\text{s,HD2}}^k &= \underbrace{\sum_{i \in \mathbb{L}} \mathbf{v}_{\text{sd},2}^{i,k} \sqrt{p_{\text{sd},2}^{i,k}} s_{\text{sd},2}^{i,k}}_{:=\tilde{\mathbf{x}}_{\text{s,HD2}}^k} + \mathbf{e}_{\text{t,s},2}, \\
\mathbf{x}_{\text{r,HD2}}^k &= \underbrace{\sum_{i \in \mathbb{L}} \mathbf{v}_{\text{rd}}^{i,k} \sqrt{p_{\text{rd}}^{i,k}} s_{\text{rd}}^{i,k}}_{:=\tilde{\mathbf{x}}_{\text{r,HD2}}^k} + \mathbf{e}_{\text{t,r}}, \quad \forall k \in \mathbb{K},
\end{aligned} \tag{31}$$

where $\mathbf{v}_{\text{sd},2}^{i,k}$ and $p_{\text{sd},2}^{i,k}$ represent the normalized precoding matrix and transmit power corresponding to the user i using sub-carrier k during the second time slot, respectively. The received signal at user i during the second time slot can be stated as

$$y_{\text{d},2}^{i,k} = \underbrace{\mathbf{h}_{\text{sd}}^{i,k} \mathbf{x}_{\text{s,HD2}}^k + \mathbf{h}_{\text{rd}}^{i,k} \mathbf{x}_{\text{r,HD2}}^k + n_{\text{d}}^{i,k}}_{:=\tilde{y}_{\text{d},2}^{i,k}} + e_{\text{r,d},2}^{i,k}, \quad \forall k \in \mathbb{K}. \tag{32}$$

⁸and similarly for $\bar{R}_{\text{sd}}^{i,k}, \bar{R}_{\text{rd}}^{i,k}$ in relation to $R_{\text{sd}}^{i,k}$ and $R_{\text{rd}}^{i,k}$.

The statistics of the distortion term can be expressed as

$$\mathbf{e}_{t,s,1}^k \sim \mathcal{CN} \left(\mathbf{0}_{N_S}, \frac{1}{K} \tilde{\Theta}_{t,s} \sum_{k \in \mathbb{K}} \text{diag} \left(\mathbb{E} \{ \tilde{\mathbf{x}}_{s,\text{HD}_1}^k (\tilde{\mathbf{x}}_{s,\text{HD}_1}^k)^H \} \right) \right), \quad (33)$$

$$\mathbf{e}_{t,s,2}^k \sim \mathcal{CN} \left(\mathbf{0}_{N_S}, \frac{1}{K} \tilde{\Theta}_{t,s} \sum_{k \in \mathbb{K}} \text{diag} \left(\mathbb{E} \{ \tilde{\mathbf{x}}_{s,\text{HD}_2}^k (\tilde{\mathbf{x}}_{s,\text{HD}_2}^k)^H \} \right) \right), \quad (34)$$

$$\mathbf{e}_{r,r}^k \sim \mathcal{CN} \left(0, \frac{\tilde{\beta}_r}{K} \sum_{k \in \mathbb{K}} \left(\mathbb{E} \{ \tilde{\mathbf{y}}_{r,\text{HD}_1}^k (\tilde{\mathbf{y}}_{r,\text{HD}_1}^k)^H \} \right) \right), \quad (35)$$

$$e_{r,d,1}^{i,k} \sim \mathcal{CN} \left(0, \frac{\tilde{\beta}_d^i}{K} \sum_{k \in \mathbb{K}} \left(\mathbb{E} \{ \tilde{\mathbf{y}}_{d,1}^k (\tilde{\mathbf{y}}_{d,1}^k)^H \} \right) \right), \quad (36)$$

$$e_{r,d,2}^{i,k} \sim \mathcal{CN} \left(0, \frac{\tilde{\beta}_d^i}{K} \sum_{k \in \mathbb{K}} \left(\mathbb{E} \{ \tilde{\mathbf{y}}_{d,2}^k (\tilde{\mathbf{y}}_{d,2}^k)^H \} \right) \right). \quad (37)$$

The achievable rate for the BS to relay link using sub-carrier k during the first time slot can be obtained as

$$R_{\text{sr},\text{HD}_1}^k = R_{\text{sr}}^k (\gamma_{\text{rd},j}^{km} = 0, p_{\text{rd}}^{j,m} = 0) \\ = \gamma_0 \log_2 \left(1 + \frac{|\hat{\mathbf{h}}_{\text{sr}}^k \mathbf{v}_{\text{sr},1}^k|^2 p_{\text{sr},1}^k}{\alpha_r^k + \sum_{m \in \mathbb{K}} \left(\gamma_{\text{sr},i}^{km} p_{\text{sr},1}^m + \sum_{j \in \mathbb{L}} \gamma_{\text{sd},j}^{km} p_{\text{sd},1}^{j,m} \right)} \right), \quad (38)$$

and the achievable information rate for the BS to user i using sub-carrier k can be formulated as

$$R_{\text{sd},\text{HD}_1}^{i,k} = R_{\text{sd}}^{i,k} (\tilde{\gamma}_{\text{rd},ij}^{km} = 0, p_{\text{rd}}^{j,m} = 0) \\ = \gamma_0 \log_2 \left(1 + \frac{|\hat{\mathbf{h}}_{\text{sd}}^{i,k} \mathbf{v}_{\text{sd},1}^{i,k}|^2 p_{\text{sd},1}^{i,k}}{\alpha_d^{i,k} + \sum_{m \in \mathbb{K}} \left(\tilde{\gamma}_{\text{sr},i}^{km} p_{\text{sr},1}^m + \sum_{j \in \mathbb{L}} \tilde{\gamma}_{\text{sd},ij}^{km} p_{\text{sd},1}^{j,m} \right)} \right). \quad (39)$$

Since there is no communication between the relay and user nodes during the first time slot, the achievable rate for relay-user links is considered to be zero, i.e., $R_{\text{rd},\text{HD}_1}^{i,k} = 0$.

Similarly, during the second time slot, the achievable rate between the BS and relay becomes zero as there is no communication between them, i.e., $R_{\text{sr},\text{HD}_2}^k = 0$. The achievable rate between the relay and user node i during the second time slot can be written as

$$R_{\text{rd},\text{HD}_2}^{i,k} = R_{\text{rd},\text{MU}}^{i,k} (\tilde{\gamma}_{\text{sr},i}^{km} = 0, p_{\text{sr}}^m = 0) \\ = \log_2 \left(1 + \frac{|\hat{\mathbf{h}}_{\text{rd}}^{i,k} \mathbf{v}_{\text{rd}}^{i,k}|^2 p_{\text{rd},2}^{i,k}}{\alpha_d^{i,k} + \sum_{m \in \mathbb{K}} \sum_{j \in \mathbb{L}} \left(\tilde{\gamma}_{\text{rd},ij}^{km} p_{\text{rd},2}^{j,m} + \tilde{\gamma}_{\text{sd},ij}^{km} p_{\text{sd},2}^{j,m} \right)} \right), \quad (40)$$

and the achievable rate between the BS and user node i during the second time slot can be written as

$$R_{\text{sd},\text{HD}_2}^{i,k} = R_{\text{sd}}^{i,k} (\tilde{\gamma}_{\text{sr},i}^{km} = 0, p_{\text{sr}}^m = 0) \\ = \log_2 \left(1 + \frac{|\hat{\mathbf{h}}_{\text{sd}}^{i,k} \mathbf{v}_{\text{sd},2}^{i,k}|^2 p_{\text{sd},2}^{i,k}}{\alpha_d^{i,k} + \sum_{m \in \mathbb{K}} \sum_{j \in \mathbb{L}} \left(\tilde{\gamma}_{\text{rd},ij}^{km} p_{\text{rd},2}^{j,m} + \tilde{\gamma}_{\text{sd},ij}^{km} p_{\text{sd},2}^{j,m} \right)} \right). \quad (41)$$

The total achievable information rate for the HD relay system for the entire communication (both the time slots) can be formulated as

$$R_{HD} = \sum_{i \in \mathbb{L}} \sum_{k \in \mathbb{K}} \left(R_{\text{sd},\text{HD}_1}^{i,k} + R_{\text{sd},\text{HD}_2}^{i,k} \right) + \min \left\{ \sum_{k \in \mathbb{K}} R_{\text{sr},\text{HD}_1}^k, \sum_{i \in \mathbb{L}} \sum_{k \in \mathbb{K}} R_{\text{rd},\text{HD}_2}^{i,k} \right\}. \quad (42)$$

In order to compare it with the FD relay, we need to take the average of the achievable rate during the two slots. As a result, the sum-rate maximization problem for the HD relay case can be written as

$$\begin{aligned} & \text{maximize} && 0.5 \left(\sum_{i \in \mathbb{L}} \sum_{k \in \mathbb{K}} \left(R_{\text{sd},\text{HD}_1}^{i,k} + R_{\text{sd},\text{HD}_2}^{i,k} \right) + t \right) \\ & \text{subject to} && \begin{aligned} & p_{\text{rd}}^{i,k} \geq 0, p_{\text{sr},1}^k \geq 0 \\ & p_{\text{sd},1}^{i,k} \geq 0, p_{\text{sd},2}^{i,k} \geq 0 \end{aligned} \\ & && \sum_{k \in \mathbb{K}} R_{\text{sr},\text{HD}_1}^k \geq t, \sum_{i \in \mathbb{L}} \sum_{k \in \mathbb{K}} R_{\text{rd},\text{HD}_2}^{i,k} \geq t, \\ & && \sum_{i \in \mathbb{L}} \sum_{k \in \mathbb{K}} p_{\text{sd},1}^{i,k} + \sum_{k \in \mathbb{K}} p_{\text{sr},1}^k \leq P_s, \sum_{i \in \mathbb{L}} \sum_{k \in \mathbb{K}} p_{\text{sd},2}^{i,k} \leq P_s, \\ & && \sum_{i \in \mathbb{L}} \sum_{k \in \mathbb{K}} p_{\text{rd},2}^{i,k} \leq P_r. \end{aligned} \quad (43)$$

The above optimization problem follows the same structure as (26). Therefore it can be solved using similar steps as in algorithm 1. Algorithm 2 provides a detailed procedure of the algorithm.

Algorithm 2 Sum-rate maximization for half-duplex relay

- 1: $a \leftarrow 0$ (set iteration number to zero)
 - 2: $p_{\text{rd},2,0}^{i,k}, p_{\text{sd},1,0}^{i,k}, p_{\text{sd},2,0}^{i,k}, p_{\text{sr},1,0}^k \leftarrow$ feasible initialization
 - 3: **repeat**
 - 4: $a \leftarrow a + 1$
 - 5: $p_{\text{rd},2}^{i,k}, p_{\text{sd},1}^{i,k}, p_{\text{sd},2}^{i,k}, p_{\text{sr},1}^k \leftarrow$ solve (43)
 - 6: $\left(p_{\text{rd},2,0}^{i,k}, p_{\text{sd},1,0}^{i,k}, p_{\text{sd},2,0}^{i,k}, p_{\text{sr},1,0}^k \right) \leftarrow \left(p_{\text{rd},2}^{i,k}, p_{\text{sd},1}^{i,k}, p_{\text{sd},2}^{i,k}, p_{\text{sr},1}^k \right)$
 - 7: **until** a stable point, or maximum number of a reached
 - 8: **return** $\{ p_{\text{rd},2}^{i,k}, p_{\text{sd},1}^{i,k}, p_{\text{sd},2}^{i,k}, p_{\text{sr},1}^k \}$
-

V. SIMULATION RESULTS

In this part, we evaluate the performance of the proposed relaying-enabled DuC scheme, as well as the proposed resource allocation strategies via numerical simulations. As the simulated setup, we consider a circular cell with BS at the center where the relay location is fixed. Since the relay is stationary and it knows from which direction it will receive the signal from the BS, the BS can communicate with the relay using a strong directive channel, i.e., the better antenna gain can be achieved between the BS and the relay. All communication channels follow an uncorrelated flat fading model at each sub-carrier. For the SI channel, we follow the characterization reported in [31], i.e., $\mathbf{h}_{rr} \sim \mathcal{CN} \left(\sqrt{\frac{\rho_{si} K_R}{1+K_R}} \mathbf{h}_0, \frac{\rho_{si}}{1+K_R} \mathbf{I}_{N_r} \right)$, where ρ_{si} is the SI channel strength, which is highly dependent on the passive isolation between the relay antenna array, and the dedicated directive fronthaul antenna for the BS-relay communication. \mathbf{h}_0 is a deterministic vector of all-1 elements and K_R is the Rician coefficient. We also assume that all users are operating within the vicinity of the relay and enjoy a line of sight (LOS) condition⁹, whereas the channels between the BS and users are assumed to obtain a LOS with the probability $P_{LOS}(d) = \min(0.018/d, 1) \times (1 - \exp(-d/0.063)) + \exp(-d/0.063)$, where d is the distance between the BS and users in km. In this regard, we adapt the model presented in 3GPP LTE specifications [33] regarding the simulated channel statistics, where the default system parameters are summarized in Table I. The overall system performance is then evaluated for

⁹It is assumed that the users will be only associated with the dedicated relay if it enjoys a LOS condition, which leads to a strong relay link quality.

different system conditions and for different design strategies, and averaged over 100 channel realizations.

Carrier center frequency and system bandwidth	2 GHz and 10MHz
Number of available sub-carrier K_{sys} and sub-carrier spacing	600 and 15kHz
Number of active sub-carriers $ \mathbb{K} $	12
Number of users $ \mathbb{L} $	4
Maximum service distance of the BS and the relay	500m and 100m,
Maximum transmit power at the BS and the relay	30dBm and 27dBm
Number of transmit antennas at the BS and the relay	32 and 16
Distance between BS and relay	400m
Receive antenna gain at the relay	20dBi
Pathloss (dB) between BS and users (d in km)	LOS: $103.4 + 24.2 \log_{10}(d)$ NLOS: $131.1 + 42.8 \log_{10}(d)$
Pathloss (dB) between BS and relay (d in km)	LOS: $100.7 + 23.5 \log_{10}(d)$
Pathloss (dB) between relay and users (d in km)	LOS: $103.8 + 20.9 \log_{10}(d)$
Shadowing standard deviation	Between BS and relay: 6dB Between BS and UE: 10dB Between relay and UE: 10dB
Thermal noise density	-174dBm/Hz
Noise figure at relay and UE	5dB and 9dB
Hardware distortion coefficient $\kappa = \beta$	-50dB
SI channel strength after SIC ρ_{si} and Rician coefficient K_R	-90dB and 10
Covariance of the CSI estimation error $(\sigma_{e,sl}^k)^2 = (\sigma_{e,rd}^k)^2 = (\sigma_{e,rd}^k)^2 = (\sigma_{e,sl}^k)^2 \forall k \in \mathbb{K}$,	-150dB

TABLE I. DEFAULT SYSTEM PARAMETERS USED FOR MULTI-USER SCENARIO

A. Comparison Benchmarks

The following performance benchmarks¹⁰ are evaluated to provide a meaningful comparison:

- **SuIC:** It represents the proposed algorithm (Algorithm 1) introduced in Section III, which consider the impact of the hardware distortion as well as the imperfect CSI¹¹.
- **DuC [DL-x%, RL-y%]:** It represents the DuC system which operate on different carrier frequencies for the DL and RL, similar to [2], therefore no SuIC at the user node. Here, x and y represent the percentage of the available sub-carriers used to communicate with the user using DL and RL, respectively. However, it uses different sub-carriers for DL and RL.
- **SuIC-ND:** It does not consider the hardware distortion (non-distortion (ND), $\kappa = \beta = 0$), i.e, a perfect hardware is assumed even though the system suffers from hardware distortions. Here, only the impact of CSI is taken into consideration [34].
- **ODL (only direct link):** This refers to the traditional downlink scenario where massive MIMO BS provides direct access to user equipments [35], i.e., there is no relay in the system.
- **ORL (only relay link):** This refers to the case where BS communicates with the user only through the relay link. There is no direct access for user to the BS, however the signal from the BS is considered as interference [36].
- **HD:** It represents the proposed algorithm (Algorithm 2) introduced in Section IV, where a HD relay is employed similar to [35]. The SuIC scheme is only utilized in the second time slot.

¹⁰Please note that, we have incorporated the impact of interference, transmit and receive impairments and parameter estimation inaccuracy (e.g., CSI error) in all links in the respective system optimization and performance analysis for all the algorithms otherwise specified.

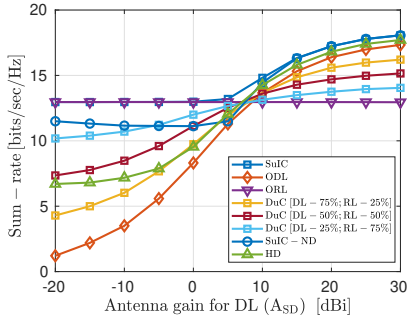
¹¹Please note that depending on the implemented technology for SIC and the deployment scenario, the potential gains of employing an FD transceiver is accompanied by accepting a higher processing and implementation complexity, associated with the required SIC capability.

B. Visualization

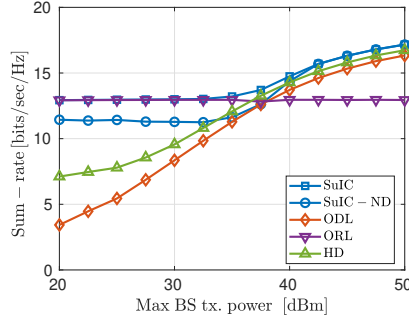
Figs. 2(a) and 2(b) portrait the system performance with respect to the strength of the direct channel between the BS and the user equipment (UE) in terms of antenna gain and transmit power at the BS, respectively. It can be observed that as the antenna gain between the BS and UE (direct link) increases, all the algorithm except ORL increases. A similar trend can be seen in the plot concerning the maximum transmit power at the BS. Another interesting observation is regarding the robustness of the SuIC against unexpected blockage. For lower values of antenna gain, for instance, in case of blockage the strength of the channel reduces drastically, the SuIC utilizes only the relay link, thereby providing better throughput compared to ODL case. As the strength of the direct link increases, SuIC utilizes both the link resulting in better performance compared to the ODL and ORL case and also becomes more robust to blockage. Moreover, for weak DL scenario, the SuIC-ND becomes worst compared to ORL and SuIC algorithms; this is because the UE is connected to BS only through an FD relay, where hardware distortion is dominant. This implies the benefit of DuC compared to single-connectivity schemes, especially in case of blockage. In Fig. 2(a), for different DuC settings, it can be observed that the system utilizing more sub-carriers for RL shows better performance at lower values of DL antenna gain. Whereas, at higher values of DL antenna gain, the system utilizing more sub-carrier for DL performs better.

Fig. 2(c) illustrates the performance of the algorithm in terms of system sum-rate for different values of transceiver inaccuracy κ dB. As it can be observed, the performance of the system decreases as the transceiver hardware distortion increases. Since the ORL operates in FD mode, the performance of ORL degrades more compared to other algorithms as the hardware-distortion increases. This shows the impact of hardware-distortion in FD system in the presence of SI. It can also be noticed that the SuIC algorithm utilizes only the relay link when the hardware inaccuracy is small. As the hardware inaccuracy increases, the performance of the SuIC also decreases. However, it can be seen that when the algorithms ORL and ODL have similar performance, the performance gain of SuIC attains maximum compared to ORL and ODL. For higher values of hardware inaccuracy, the RL is severely affected by hardware distortion due to SI, the SuIC opts the DL, thereby reducing its impact. Furthermore, the proposed algorithm (SuIC) always performs better compared to SuIC-ND algorithm. This indicates that the consideration of hardware-distortion in designing the system will improve the overall performance of the system.

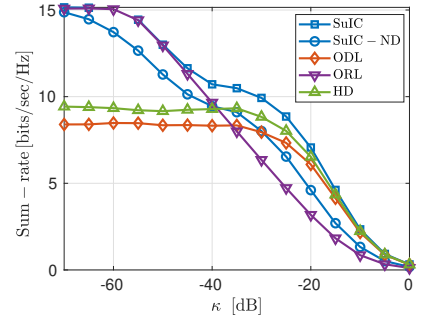
In Fig. 2(d), the impact of the UE receiver noise in the system performance is depicted. As expected, the sum-rate of the system decreases as the receiver noise at the UE increases. However, the performance gain of SuIC compared to SuIC-ND becomes more for higher values of UE receiver noise. Since the SuIC utilizes the relay link where the hardware distortion becomes dominant due to SI. Furthermore, the performance of the system is evaluated with respect to the channel estimation error in Fig. 2(e). A similar trend can be observed that the performance of all the algorithm degrades as the channel esti-



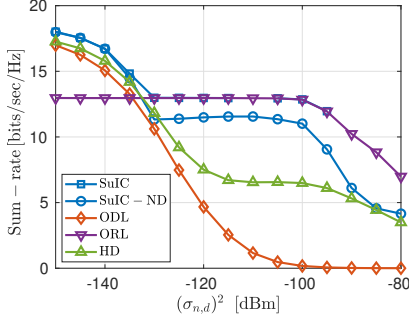
(a) Sum-rate vs. Antenna Gain between BS and UE



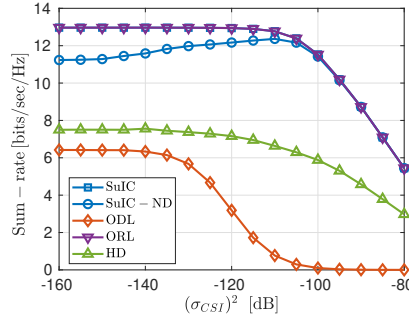
(b) Sum-rate vs. Maximum Transmit Power at BS



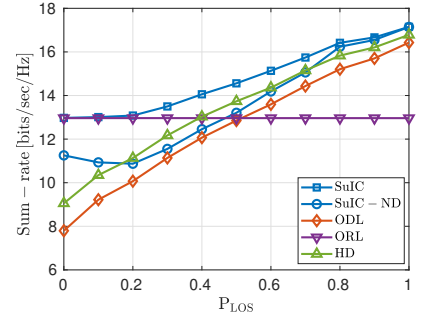
(c) Sum-rate vs. Hardware Inaccuracy



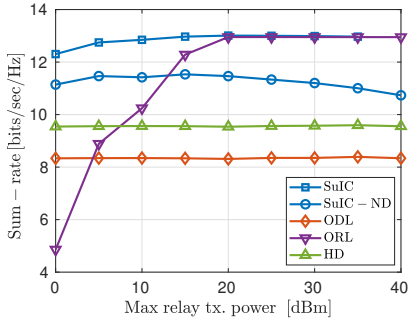
(d) Sum-rate vs. Receiver Noise at the UE



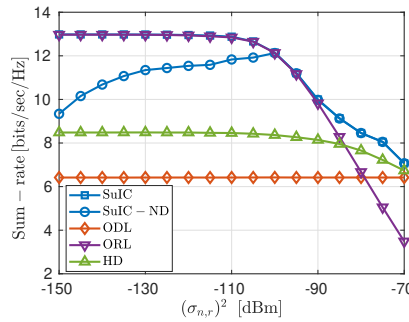
(e) Sum-rate vs. Channel Estimation Error



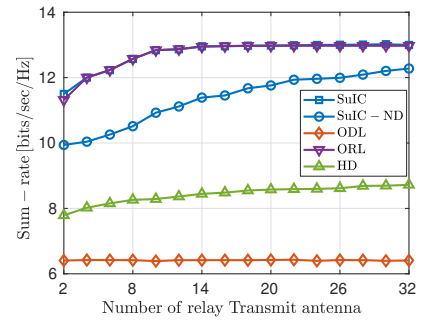
(f) Sum-rate vs. Probability of LOS between BS and UE



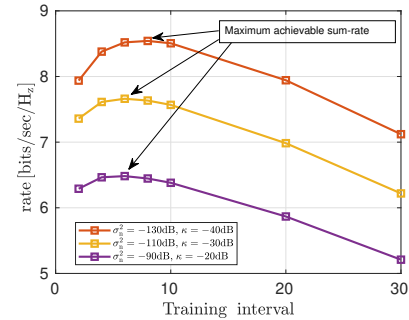
(g) Sum-rate vs. Maximum Relay Transmit Power



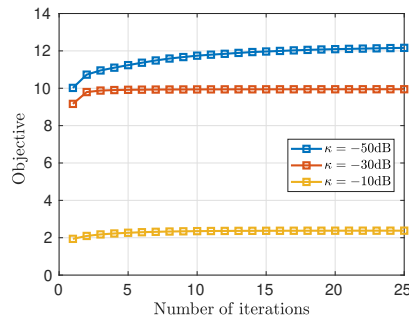
(h) Sum-rate vs. Receiver Noise at the Relay



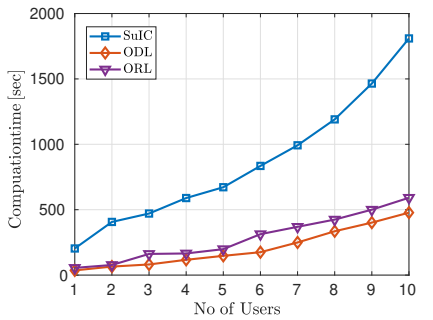
(i) Sum-rate vs. Number of Relay Transmit Antenna



(j) Sum-rate vs Estimation time (training) interval.



(k) Average Convergence Behavior of SuIC algorithm



(l) Computation time vs Number of Users.

Fig. 2. Sum-rate for Different System Parameters

mation error increases. For small values of channel estimation error, the hardware distortion becomes dominant, thus resulting in better performance of SuIC algorithm compared to the SuIC-ND algorithm. It can also be observed that as the channel estimation error increases the ODL algorithm degrades more compared to other algorithms. This is due to the fact that the direct link is weak compared to the relay link.

In Fig. 2(f), the performance of the system is evaluated with respect to the probability of LOS (P_{LOS}) of the direct channel between the BS and the UE. As it can be clearly observed, the performance of all the algorithms except for ORL increases as P_{LOS} increases. Another interesting observation is that the performance gain between the SuIC and SuIC-ND reduces as P_{LOS} increases since the SuIC algorithm uses the direct link when BS has LOS with its UEs, i.e., P_{LOS} has a higher value.

In Figs. 2(g) to 2(i), the system performance is evaluated for different parameters of the relay. Fig. 2(g) plots the performance of the system with respect to the maximum transmit power available at the relay. As expected, the performance of all the algorithms except ODL improves as the maximum transmit power available at the relay increases. A similar trend in the performance of the system is observed for the different number of transmit antenna used at the relay in Fig. 2(i). Furthermore, in Fig. 2(h), the performance of the system is evaluated for different values of receiver noise at the relay. The performance of all the algorithms except ODL degrades as the receiver noise at the relay increases. However, as the receiver noise decreases, the SuIC-ND performance degrades compared to the SuIC, due to the fact that the hardware distortion becomes dominant when the receiver noise becomes small. It can also be noticed that, as the receiver noise at the relay increases, the performance of ORL decreases while the performance of ODL remains almost similar. The SuIC shows slightly better performance compared to ORL for higher values of receiver noise at the relay as it also utilizes the DL.

The Fig.2(j) shows the performance of the SuIC algorithm w.r.t the training interval (T_{train}) for different values of noise and hardware distortion ($\kappa = \beta$). Here, we choose $T_{\text{tot}} = 100$ symbols. It can be clearly seen that for small values of training interval, the system performance in terms of sum-rate increases along with training interval. After a certain point (maximum achievable sum-rate) the sum-rate decreases as the training interval increases, this is because the time duration for the data transmission decreases as the training interval increases. Another interesting observation is that for higher noise and hardware distortion values, maximum achievable sum-rate attains with lesser training interval. This is due to the fact that, as the noise and hardware distortion are high, it is better to allocate more resources for data transmission than channel estimation.

The Fig.2(k) shows the average convergence behavior of our proposed SuIC algorithm with equal power initialization for different values of hardware inaccuracy κ dB. It can be observed that the algorithm converges within 10-25 iterations. As expected, it can be seen that the objective has a higher value for smaller hardware inaccuracy. Furthermore, Fig.2(l) shows that the computational complexity of the algorithm in terms

of computation time¹² with equal power initialization with respect to number of users. As expected, as the number of users increases, the computational complexity of the algorithms also increases. It can also be observed that the SuIC algorithm is more computational complex than ODL and ORL case, because of DuC.

VI. CONCLUSION

In this paper, we studied the downlink of a cellular communication network, where DuC at the end-users is enabled with the assistance of an FD mMIMO relay. As a result, the downlink communication data can be interchangeably loaded to separate sub-carriers, employing an MC strategy, or to the different available links, i.e., direct or the FD relay link, employing the non-orthogonal SuIC at the receiver. Numerical simulations show that the proposed SuIC approach reaches a higher performance compared to the single-connectivity and HD schemes, and also implies the importance of the hardware-distortion aware system, especially as the hardware accuracy degrades.

The proposed dual-connectivity scheme can be explicitly used to gain robustness against the path blockages, when the statistics of such occurrence can be extracted from data (since these events are occurring in short time periods). Hence, it is the intention of our future work to augment an online learning-based beam and power adjustment method to the current setup, in order to utilize the proposed DuC scheme for combating the occasional path-blockage situations.

APPENDIX A PROOF OF LEMMA II.1

The time domain statistical independence $e_{t,l}(t) \perp v_l(t)$ and $e_{t,l}(t) \perp e_{t,l'}(t)$, and the linear nature of the transformation (8) are also applicable to the statistical independence properties at the transformed unitary domain. Similarly, the Gaussian and zero-mean properties for $e_{t,l}^k$ becomes a linearly weighted sum of the zero-mean Gaussian values $e_{t,l}(mT_s)$. The variance of $e_{t,l}^k$ can hence be obtained as

$$\begin{aligned}
 \mathbb{E} \left\{ |e_{t,l}^k|^2 \right\} &= \mathbb{E} \left\{ \left(\sum_{m=0}^{N-1} e_{t,l}(mT_s) q_{k,m}^* \right) \times \left(\sum_{n=0}^{N-1} e_{t,l}^*(nT_s) q_{k,n} \right) \right\} \\
 &= \sum_{m=0}^{N-1} \sum_{n=0}^{N-1} \mathbb{E} \left\{ e_{t,l}(mT_s) e_{t,l}^*(nT_s) \right\} q_{k,m}^* q_{k,n} \\
 &= \sum_{m=0}^{N-1} \mathbb{E} \left\{ e_{t,l}(mT_s) e_{t,l}^*(mT_s) \right\} q_{k,m} q_{k,m}^* (e_{t,l}(t) \perp e_{t,l}(t')) \\
 &= \kappa_l \mathbb{E} \left\{ |v_l(t)|^2 \right\} \quad (\text{from (7) and } \sum_{m=0}^{N-1} q_{k,m} q_{k,m}^* = 1) \\
 &= \frac{\kappa_l}{K} \sum_{m=1}^K \mathbb{E} \left\{ |v_l^m|^2 \right\} \quad (\text{Parseval's Theorem on energy conversation}).
 \end{aligned} \tag{44}$$

Similarly, the proof to the receiver characterization can be obtained.

¹²The reported computation time is obtained using an Intel Core i7-4790S processor with a clock rate of 3.2 GHz and 16 GB RAM. We use MATLAB 2019a on a 64-bit operating system.

REFERENCES

- [1] V. Radhakrishnan, O. Taghizadeh, and R. Mathar, "Full-Duplex Relaying: Enabling Dual Connectivity via Impairments-Aware Successive Interference Cancellation," in *WSA 2020; 24th International ITG Workshop on Smart Antennas*, Feb 2020, pp. 1–6.
- [2] 3GPP, "Study on Small Cell enhancements for E-UTRA and E-UTRAN; Higher layer aspects," 3rd Generation Partnership Project (3GPP), Technical report (TR) 36.331, Dec 2013, version 12.0.0.
- [3] —, "Technical specification group radio access network; NR; physical layer; general description (Release 15)," 3rd Generation Partnership Project (3GPP), Technical report (TR) 38.201, 2017, version 1.0.0.
- [4] P. Guan, D. Wu, T. Tian, J. Zhou, X. Zhang, L. Gu, A. Benjebbour, M. Iwabuchi, and Y. Kishiyama, "5G Field Trials: OFDM-Based Waveforms and Mixed Numerologies," *IEEE Journal on Selected Areas in Communications*, vol. 35, no. 6, pp. 1234–1243, 2017.
- [5] S. M. R. Islam, N. Avazov, O. A. Dobre, and K.-s. Kwak, "Power-Domain Non-Orthogonal Multiple Access (NOMA) in 5G Systems: Potentials and Challenges," *IEEE Communications Surveys and Tutorials*, vol. 19, no. 2, p. 721–742, 2017.
- [6] R. Antoniolli, G. Parente, C. Silva, D. Sousa, E. Rodrigues, T. Maciel, and F. Cavalcanti, "Dual Connectivity for LTE-NR Cellular Networks: Challenges and Open Issues," *Journal of Communication and Information Systems*, vol. 33, no. 1, Aug. 2018.
- [7] O. N. C. Yilmaz, O. Teyeb, and A. Orsino, "Overview of LTE-NR Dual Connectivity," *IEEE Communications Magazine*, vol. 57, no. 6, pp. 138–144, 2019.
- [8] T. Mumtaz, S. Muhammad, M. I. Aslam, and N. Mohammad, "Dual Connectivity-Based Mobility Management and Data Split Mechanism in 4G/5G Cellular Networks," *IEEE Access*, vol. 8, pp. 86 495–86 509, 2020.
- [9] A. Zakrzewska, D. López-Pérez, S. Kucera, and H. Claussen, "Dual connectivity in LTE HetNets with split control- and user-plane," in *2013 IEEE Globecom Workshops (GC Wkshps)*, Dec 2013, pp. 391–396.
- [10] C. Rosa, K. Pedersen, H. Wang, P. Michaelsen, S. Barbera, E. Malkamäki, T. Henttonen, and B. Sébire, "Dual connectivity for LTE small cell evolution: functionality and performance aspects," *IEEE Communications Magazine*, vol. 54, no. 6, pp. 137–143, June 2016.
- [11] C. K. Thomas, B. Clerckx, L. Sanguinetti, and D. Slock, "A Rate Splitting Strategy for Mitigating Intra-Cell Pilot Contamination in Massive MIMO," in *2020 IEEE International Conference on Communications Workshops (ICC Workshops)*, 2020, pp. 1–6.
- [12] A. Papazafeiropoulos, B. Clerckx, and T. Ratnarajah, "Rate-Splitting to Mitigate Residual Transceiver Hardware Impairments in Massive MIMO Systems," *IEEE Transactions on Vehicular Technology*, vol. 66, no. 9, pp. 8196–8211, Sep. 2017.
- [13] M. Hojeij, C. A. Nour, J. Farah, and C. Douillard, "Joint Resource and Power Allocation Technique for Downlink Power-Domain Non-Orthogonal Multiple Access," in *2018 IEEE Conference on Antenna Measurements Applications (CAMA)*, Sep. 2018, pp. 1–4.
- [14] X. Xia, D. Zhang, K. Xu, W. Ma, and Y. Xu, "Hardware Impairments Aware Transceiver for Full-Duplex Massive MIMO Relaying," *IEEE Transactions on Signal Processing*, vol. 63, no. 24, pp. 6565–6580, Dec 2015.
- [15] W. Xie, X. Xia, Y. Xu, K. Xu, and Y. Wang, "Massive MIMO full-duplex relaying with hardware impairments," *Journal of Communications and Networks*, vol. 19, no. 4, pp. 351–362, August 2017.
- [16] A. Shojaefard, K. Wong, M. D. Renzo, G. Zheng, K. A. Hamdi, and J. Tang, "Massive MIMO-Enabled Full-Duplex Cellular Networks," *IEEE Transactions on Communications*, vol. 65, no. 11, pp. 4734–4750, Nov 2017.
- [17] L. Chen, F. R. Yu, H. Ji, B. Rong, and V. C. M. Leung, "Power allocation in small cell networks with full-duplex self-backhauls and massive MIMO," *Wireless Networks*, vol. 24, no. 4, pp. 1083–1098, May 2018. [Online]. Available: <https://doi.org/10.1007/s11276-016-1381-1>
- [18] L. Li, J. He, L. Yang, Z. Han, M. Pan, W. Chen, H. Zhang, and X. Li, "Spectral- and Energy-Efficiency of Multi-Pair Two-Way Massive MIMO Relay Systems Experiencing Channel Aging," *IEEE Access*, vol. 7, pp. 46 014–46 032, 2019.
- [19] D. Wang, M. Wang, P. Zhu, J. Li, J. Wang, and X. You, "Performance of Network-Assisted Full-Duplex for Cell-Free Massive MIMO," *IEEE Transactions on Communications*, vol. 68, no. 3, pp. 1464–1478, 2020.
- [20] M. Zaher and A. El-Mahdy, "Two-Way Full-Duplex Massive MIMO Relaying with Correlated Multi-Antenna User Pairs," in *2019 5th International Conference on Frontiers of Signal Processing (ICFSP)*, 2019, pp. 57–61.
- [21] S. Jin, D. Yue, and H. H. Nguyen, "Power Scaling Laws of Massive MIMO Full-Duplex Relaying With Hardware Impairments," *IEEE Access*, vol. 6, pp. 40 860–40 882, 2018.
- [22] O. Taghizadeh, V. Radhakrishnan, A. C. Cirik, R. Mathar, and L. Lampe, "Hardware Impairments Aware Transceiver Design for Bidirectional Full-Duplex MIMO OFDM Systems," *IEEE Transactions on Vehicular Technology*, vol. 67, no. 8, pp. 7450–7464, Aug 2018.
- [23] B. R. Marks and G. P. Wright, "Technical Note—A General Inner Approximation Algorithm for Nonconvex Mathematical Programs," *Operations Research*, vol. 26, no. 4, pp. 681–683, 1978.
- [24] D. W. K. Ng, E. S. Lo, and R. Schober, "Dynamic Resource Allocation in MIMO-OFDMA Systems with Full-Duplex and Hybrid Relaying," *IEEE Transactions on Communications*, vol. 60, no. 5, pp. 1291–1304, May 2012.
- [25] A. C. Cirik, Y. Rong, and Y. Hua, "Achievable Rates of Full-Duplex MIMO Radios in Fast Fading Channels With Imperfect Channel Estimation," *IEEE Transactions on Signal Processing*, vol. 62, no. 15, pp. 3874–3886, Aug 2014.
- [26] B. P. Day, A. R. Margetts, D. W. Bliss, and P. Schniter, "Full-Duplex MIMO Relaying: Achievable Rates Under Limited Dynamic Range," *IEEE Journal on Selected Areas in Communications*, vol. 30, no. 8, pp. 1541–1553, 2012.
- [27] B. P. Day, D. W. Bliss, A. R. Margetts, and P. Schniter, "Full-duplex bidirectional MIMO: Achievable rates under limited dynamic range," in *2011 Conference Record of the Forty Fifth Asilomar Conference on Signals, Systems and Computers (ASILOMAR)*, Nov 2011, pp. 1386–1390.
- [28] W. Namgoong, "Modeling and analysis of nonlinearities and mismatches in AC-coupled direct-conversion receiver," *IEEE Transactions on Wireless Communications*, vol. 4, no. 1, pp. 163–173, Jan 2005.
- [29] G. Santella and F. Mazzenga, "A hybrid analytical-simulation procedure for performance evaluation in M-QAM-OFDM schemes in presence of nonlinear distortions," *IEEE Transactions on Vehicular Technology*, vol. 47, no. 1, pp. 142–151, Feb 1998.
- [30] H. Suzuki, T. V. A. Tran, I. B. Collings, G. Daniels, and M. Hedley, "Transmitter Noise Effect on the Performance of a MIMO-OFDM Hardware Implementation Achieving Improved Coverage," *IEEE Journal on Selected Areas in Communications*, vol. 26, no. 6, pp. 867–876, August 2008.
- [31] M. Duarte, C. Dick, and A. Sabharwal, "Experiment-Driven Characterization of Full-Duplex Wireless Systems," *IEEE Transactions on Wireless Communications*, vol. 11, no. 12, pp. 4296–4307, December 2012.
- [32] S. Boyd and L. Vandenberghe, *Convex Optimization*. New York, NY, USA: Cambridge University Press, 2004.
- [33] 3GPP, "Evolved Universal Terrestrial Radio Access (E-UTRA); Further advancements for E-UTRA physical layer aspects," 3rd Generation Partnership Project (3GPP), Technical report (TR) 36.814, March 2010, version 2.0.0.
- [34] X.-X. Nguyen and D.-T. Do, "System Performance of Cooperative NOMA with Full-Duplex Relay over Nakagami-m Fading Channels," *Mobile Information Systems*, vol. 2019, p. 7547431, Mar 2019.
- [35] A. Bonfante, L. Galati Giordano, D. López-Pérez, A. Garcia-Rodriguez, G. Geraci, P. Baracca, M. M. Butt, and N. Marchetti, "5G Massive MIMO Architectures: Self-Backhauled Small Cells Versus Direct Access," *IEEE Transactions on Vehicular Technology*, vol. 68, no. 10, pp. 10 003–10 017, 2019.
- [36] E. Chen, M. Tao, and N. Zhang, "User-Centric Joint Access-Backhaul Design for Full-Duplex Self-Backhauled Wireless Networks," *IEEE Transactions on Communications*, vol. 67, no. 11, pp. 7980–7993, 2019.